Journal of Theoretical Biology 309 (2012) 159–175

Contents lists available at SciVerse ScienceDirect

Journal of Theoretical Biology

journal homepage: www.elsevier.com/locate/yjtbi

Mathematical modelling of tooth demineralisation and pH profiles in dental plaque

Olga Ilie*, Mark C.M. van Loosdrecht, Cristian Picioreanu

Delft University of Technology, Department of Biotechnology, Environmental Biotechnology Group, The Netherlands

HIGHLIGHTS

- A one-dimensional time-dependent mathematical model of dental plaque is presented.
- The model integrates (bio)chemical processes in the plaque with tooth demineralisation.
- The model describes typical Stephan curves in different conditions.
- On short term storage compounds might not have a negative effect on demineralisation.
- Slow drinking of sugar containing drinks proves to be more harmful than gulping.

ARTICLE INFO

Article history:
Received 17 April 2012
Received in revised form
22 May 2012
Accepted 22 May 2012
Available online 8 June 2012

Keywords:
Numerical model
Oral biofilms
Stephan curves
Enamel dissolution

ABSTRACT

A mathematical model of dental plaque has been developed in order to investigate the processes leading to dental caries. The one-dimensional time-dependent model integrates existing knowledge on biofilm processes (mass transfer, microbial composition, microbial conversions and substrate availability) with tooth demineralisation kinetics. This work is based on the pioneering studies of Dibdin who, nearly two decades ago, build a mathematical model roughly describing the metabolic processes taking place in dental plaque. We extended Dibdin's model with: multiple microbial species (aciduric and non-aciduric *Streptococci*, *Actinomyces* and *Veillonella*), more metabolic processes (i.e., aerobic and anaerobic glucose conversion, low and high glucose uptake affinity pathways, formation and consumption of storage compounds), ion transport by Nernst–Planck equations, and we coupled the obtained pH and chemical component gradients inside the plaque with tooth demineralisation. The new model implementation was complemented with faster and more rigorous numerical methods for the model solution. Model results confirm the protective effect of *Veillonella* due to lactate consumption. Interestingly, on short term, the storage compounds may not necessarily have a negative effect on demineralisation. Individual feeding patterns can also be easily studied with this model. For example, slow ("social") consumption of sugar-containing drinks proves to be more harmful than drinking the same amount over a short period of time.

1. Introduction

Dental caries is currently one of the most widespread conditions associated with oral hygiene. The term dental caries is used to describe the results – signs and symptoms – of a localised chemical dissolution of the tooth surface caused by metabolic events taking place in the biofilm (dental plaque) covering the affected area (Fejerskov and Kidd, 2008). Dental enamel consists of approximately 99% (dry weight) microscopic calcium phosphate crystals (called *rods*) resembling the mineral hydroxyapatite (HAP), $Ca_5(PO_4)_3(OH)$, together with impurities such as carbonate, sodium, fluoride and other ions. The inter-rod space in the enamel is filled with water and organic matter, allowing diffusion of protons and other ions through the enamel.

Carbohydrate consumption by microorganisms present in the dental plaque leads to organic acid production, which causes an acidic pH in the plaque. This triggers a variation in the degree of saturation of plaque liquid with respect to HAP. Dental caries is the direct consequence of the resulting dissolution of HAP due to the decreased pH. The caries formation process is extended over a long time span, which correlated with the conditions present in the mouth, makes it very difficult for *in vivo* studies. Currently, the *in vitro* studies are limited mainly by two factors: (1) the difficulty of creating HAP crystals with a similar structure to the natural enamel, for the studies using artificial teeth. This problem can be surpassed using extracted human or animal teeth (Larsen and Pearce, 1992; Featherstone et al., 1979; Lippert et al., 2004); (2) the long time periods required to develop caries reproducing

* Corresponding author. Tel.: +31 15 27 89175; fax: +31 15 27 82355.
E-mail address: o.ilie@tudelft.nl (O. Ilie).

0022-5193/$ - see front matter © 2012 Elsevier Ltd. All rights reserved.
http://dx.doi.org/10.1016/j.jtbi.2012.05.024

the conditions present in the mouth: acid attacks during eating and drinking (resulting in demineralisation) interposed with fasting periods (with the potential of remineralisation). Therefore, continuous acid attack is often used in experimental studies (Larsen and Pearce, 1992; Lippert et al., 2004; Margolis and Moreno, 1992). Mathematical modelling offers a different research perspective by surmounting some of the problems the experimental studies are facing, such as the long time period required for the development of the caries from the subclinical level until the clinically visible caries. Using numerical tools it is possible to create a controlled environment in which reality is simplified to the relevant aspects for the problem to be studied. This is also offering the possibility of easily adding or removing different physical, chemical or biological processes in order to study in separation their influence on the system which, from an experimental point of view can be very difficult to achieve.

Because of its high relevance, dental caries problem has been intensively studied and, as soon as the computational power allowed it, the first mathematical models for tooth demineralisation (Holly and Grey, 1968; Zimmerman, 1966a, b, c; Fox et al., 1978) have been developed. As the experimental studies over the years offered more insight into the problem, new and more sophisticated numerical models emerged (Van Dijk et al., 1979; Ten Cate, 1982). These models are dealing exclusively with the processes taking place in the enamel, while the plaque itself is not considered. Higuchi et al. (1970) developed a first mathematical model accounting for dental plaque, diffusion of glucose, glucose conversion to lactate and enamel demineralisation. Major limitations of this model are the steady state assumption, the constant glucose concentration in saliva and the lactic acid production not inhibited at low pH.

Dibdin and Reece (1984) developed the first model in a series of mathematical models of dental plaque (Dawes and Dibdin, 1986; Dibdin, 1990a, b, 1997; Dibdin et al., 1995; Dibdin and Dawes, 1998). These models aimed at calculating the one-dimensional and, further (Dawes, 1989), the two-dimensional pH profiles in the depth of dental biofilms, as a consequence of the metabolic processes taking place in the dental plaque when sucrose is provided. Moreover, the variation of plaque pH in time (the so-called Stephan curves; Dawes and Dibdin, 1986; Fejerskov and Kidd, 2008) in different conditions was also explained by these models. Surprisingly, development of these models has not been continued during the recent years. We decided to extend Dibdin's work by making advantage of both increased understanding of plaque processes and function and of computational resources. In this paper we describe the development of a model integrating complex metabolic, chemical and mass transfer processes occurring in the dental plaque with the rate of enamel demineralisation. The main improvements in the current model in respect with the previous work of Dawes and Dibdin are summarised in Table 1. Our aim was to (1) investigate the process of caries formation in a more quantitative and structured manner, (2) identify critical parameters playing a role in caries formation and (3) guide new research in respect with relevant and not understood aspects of caries formation.

Table 1
Comparison of current model with the model of Dawes and Dibdin, 1986.

Current model	Dibdin's models
Ion migration rate with Nernst–Planck equation	Charge balancing
Multiple bacterial species (aciduric and non-aciduric *Streptococcus*, *Actinomyces*, *Veillonella*)	One generic species (presumably aciduric *Streptococcus*)
Polysaccharide (polyglucose) storage and consumption	Only polysaccharide storage
Five acids: lactic, acetic, propionic, formic, succinic	Two acids: lactic, to account for strong organic acids, and acetic, to account for weak acids
Aerobic and anaerobic metabolism included	Only anaerobic metabolism
Reliable demineralisation kinetics for the tooth	Enamel is assumed to be inert

2. Model description

The mathematical model considers planar dental plaque geometry with only one-dimensional gradients of solute concentration from the saliva perpendicular to the tooth surface. Multiple microbial and chemical species are taken into account together with a selection of the most relevant metabolic and chemical processes that have the potential to influence significantly the plaque pH.

2.1. Components

The model has to describe the chemical interactions between several types of microorganisms present in the dental plaque via different substrates and metabolic products. Therefore, in the present model we first distinguish between microbial components and chemical components. The microbial components are immobile and they are the constituents of the dental plaque. Further, the chemical components can be divided into mobile and immobile. While we assume that the microbial and the immobile chemical components are present only in the dental plaque, the mobile chemical ones exist both in the saliva and dental plaque. In the following sections a detailed description of the model components and processes in which they are involved is provided.

2.1.1. Microbial components

One of the goals of this study was to find out whether it is relevant to include multiple microbial components performing a series of bio-transformations or it is sufficient just to lump all active microbial species into a single generic component (such as in the reference work of Dibdin, Dawes and Dibdin, 1986; Dibdin, 1990a, b; Dibdin, 1997). There is vast amount of literature reporting studies on the microbial composition of dental plaque (e.g., Fejerskov and Kidd, 2008; Marsh et al., 2009; Ritz, 1967; Bowden, 2000; Takahashi and Nyvad, 2008; Filoche et al., 2010). Among the main microbial groups present and active in dental plaque are: *Streptococcus*, *Actinomyces*, *Lactobacillus*, *Veillonella*, *Propionibacterium*, *Bifidobacterium* and *Capnocytophaga* (Hojo et al., 2009). In order to keep the model within reasonable limits of complexity, while still considering the dominant microorganisms in the plaque, the following microbial groups have been selected as plaque constituents for the current study:

- *Streptococcus* is a facultative anaerobic bacterium that can represent up to 85% (Fejerskov and Kidd, 2008; Marsh et al., 2009) of the organisms present in dental plaque. Two *Streptococcus* categories must be differentiated because they have different niches in the dental plaque:
- non-aciduric *Streptococci* (*S. milleri*, *S. sanguis*, *S. salivarius* etc.) living in the near neutral pH range, denoted by STN in this model, are the majority.
- aciduric *Streptococci* (*S. mutans*, *S. sobrinus*) active until pH as low as 4.5 (Hamilton and Buckley, 1991; Bowden, 2000), symbolized by STA, appear as a minority group in dental plaque. Even though STA are usually accounting for a small percentage of the plaque (between 0% and 23%, Marsh et al., 2009), their influence seems to be important for the purpose of this study, since an increase in the concentration of aciduric *Streptococci* is usually associated with the appearance of dental caries around

pH 5.5. Therefore, both STA and STN have to be included in the dental plaque model.

- *Actinomyces* is the second most present microbial group in the dental plaque (up to 45%, Fejerskov and Kidd, 2008; Marsh et al., 2009) and it is also facultative anaerobe (Ritz, 1967). In the model we represented all *Actinomyces* as a generic group, ACT, taking into account the main glucose conversions occurring in this genus.
- *Veillonella* are strictly anaerobes and they are the third most abundant group of microorganisms present in mature oral biofilms (sometimes up to 40%, Fejerskov and Kidd, 2008; Marsh et al., 2009). The *Veillonella* are also represented in the model as a lumped metabolic group, VEL.

We neglected several other microbial groups reported as being possibly important. Among these, *Lactobacillus* is an anaerobe usually present in low amounts in the plaque and especially in the advanced stages of caries formation process (Loesche, 1986).

Microbial components are described by their concentration in the plaque $C_{X,i}$ [(kg dry biomass) (m^{-3} plaque)]. For simplification, in the current study we did not include microbial growth, neither a layered plaque structure. It was considered that during the limited period of time studied by the present simulations (~2–3 h), the plaque thickness and the plaque microbial composition would remain relatively constant. The plaque composition was assumed (Table 2) based on the values reported in Marsh et al. (2009) and Fejerskov and Kidd (2008). There is therefore no microbial state variable whose distribution in space and time must be computed by the model.

Table 2
Microbial components in the model and their constant concentrations in dental plaque (assumed cf. Fejerskov and Kidd, 2008 and Marsh et al., 2009).

Named	Symbol	Concentration [(kg dry biomass) (m^{-3} plaque)]	Concentration [mass %]
Aciduric *Streptococcus*	$C_{X,STA}$	4	5
Non-aciduric *Streptococcus*	$C_{X,STN}$	36	45
Actinomyces	$C_{X,ACT}$	32	40
Veillonella	$C_{X,VEL}$	8	10

Table 3
Mobile chemical species and their associated properties in the current model.

Name	Symbol	Formula	Charge	Diffusion coefficient[a]		Initial concentration in saliva film and plaque	
				[10^{-9} m^2 s^{-1}]	Reference	[mmol L^{-1}]	Reference/calculation
Acetate	Ace–	$C_2H_3O_2^-$	−1	1.38	Cussler (2009) Vanýsek (2001)	0	Equilibrium, $C_{Ace,tot}=0$
Acetic acid	AceH	$C_2H_4O_2$	0	1.64	Cussler (2009) Vanýsek (2001)	0	Equilibrium
Formate	For–	CHO_2^-	−1	1.84	Vanýsek (2001)	0	Equilibrium, $C_{For,tot}=0$
Formic acid	ForH	CH_2O_2	0	1.79	Cussler (1984)	0	Equilibrium
Lactate	Lac–	$C_3H_5O_3^-$	−1	1.31	Vanýsek (2001)	0	Equilibrium, $C_{Lac,tot}=0$
Lactic acid	LacH	$C_3H_6O_3$	0	1.41	Assumed	0	Equilibrium
Propionate	Pro–	$C_3H_5O_2^-$	−1	1.20	Cussler (2009) Vanýsek (2001)	0	Equilibrium, $C_{Pro,tot}=0$
Propionic acid	ProH	$C_3H_6O_2$	0	1.34	Cussler (1984)	0	Equilibrium
Succinate	Suc2–	$C_4H_4O_4^{2-}$	−2	0.99	Vanýsek (2001)	0	Equilibrium, $C_{Suc,tot}=0$
Hydrogen succinate	Suc–	$C_4H_5O_4^-$	−1	1.10	Assumed	0	Equilibrium
Succinic acid	SucH	$C_4H_6O_4$	0	1.19	Cussler (1984)	0	Equilibrium
Bicarbonate	HCO3–	CHO_3^-	−1	1.50	Vanýsek (2001)	4.17	Equilibrium, $C_{CO2,tot}=5.1$ [mmol L^{-1}], Marsh et al. (2009)
Carbon dioxide	CO2	CO_2	0	2.43	Cussler (2009)	0.93	Equilibrium
Hydrogen phosphate	Pho2–	HPO_4^{2-}	−2	0.96	Vanýsek (2001)	2.06	Equilibrium, $C_{Pho,tot}=5.4$ [mmol L^{-1}], Fejerskov and Kidd (2008)
Dihydrogen phosphate	Pho–	$H_2PO_4^-$	−1	1.22	Vanýsek (2001)	3.34	Equilibrium
Hydroxyl	HO–	HO^-	−1	6.7	Cussler (2009) Vanýsek (2001)	10^{-4}	Equilibrium
Proton	H+	H^+	+1	11.81	Cussler (2009) Vanýsek (2001)	10^{-4}	Fejerskov and Kidd (2008)
Calcium	Ca2+	Ca^{2+}	+2	1.00	Cussler (2009) Vanýsek (2001)	0.04	Equilibrium, $C_{Ca2+,tot}=1.32$ [mmol L^{-1}], Fejerskov and Kidd (2008)
Anion (chloride)	Cl–	Cl^-	−1	2.57	Cussler (2009) Vanýsek (2001)	40	Fejerskov and Kidd (2008)
Cation (potassium)	K+	K^+	+1	2.49	Cussler (2009) Vanýsek (2001)	$C_{s,K+}=$ 49 $C_{p,K+}=$ 80.86	Charge balance in saliva Charge balance in plaque
Oxygen	O2	O_2	0	2.66	Cussler (2009)	0.15	Assumed
Glucose	Glu	$C_6H_{12}O_6$	0	0.85	Vanýsek (2001)	0.07	Van der Hoeven et al. (1990)
Ethanol	Eth	C_2H_6O	0	1.57	Vanýsek (2001)	0	Assumed

[a] The values of diffusion coefficients are calculated at 37 °C based on the values at 25 °C given in references. The diffusion coefficients increase with 2% per temperature degree (Vanýsek, 2001).

2.1.2. Chemical components

The chemical model components are chemical species relevant for describing the cariogenic effect of dental plaque. We distinguish between mobile and immobile (fixed) chemical species. Each mobile chemical species (Table 3) is characterised by a constant diffusion coefficient D_i and charge z_i, and it is described by a state variable, concentration C_i, changing in time in saliva and at different depths in the dental plaque. In the first place, substrates for the considered microbial components must be included, such as glucose (for aciduric and non-aciduric *Streptococcus* and *Actinomyces*) and lactate (for *Veillonella*), plus the dissolved oxygen. Secondly, the organic acids produced in anaerobic fermentations or aerobic conversions (e.g., lactic, acetic, propionic, succinic, formic) are taken into account because they are the main cause of caries formation. Thirdly, enamel ions such as calcium and phosphate are included to be able to calculate the enamel dissolution rates. In addition, other background electrolytes, cations (K^+) and anions (Cl^-) are needed for charge balancing. The final group of chemical components is needed for speciation in acid–base equilibria (the base of pH and charge balance calculations), namely the main dissociation/association species of each chemical component (e.g., lactic acid and lactate ion, proton and hydroxyl ions, carbon dioxide and bicarbonate ions, etc.).

There are two types of immobile chemical components in the plaque. First, the "surface species" account for the buffering capacity of the dental plaque (Shellis and Dibdin, 1988; Hong and Brown, 2006). They are functional groups bound to the bacterial cell wall or extracellular polymers and they participate in the ion speciation and charge balancing. Different chemical compounds stored within the microbial cells, such as a generic polyglucose component, are also accounted for. The immobile chemical components (Table 4) are characterised by a concentration variable in time and at different depths in the plaque.

2.2. Processes

Each of the microbial groups considered active in dental plaque model carries out several metabolic processes, according to different pathways (e.g., aerobic, anaerobic, low or high glucose). These pathways will be called here *biological reactions*. In addition, because the main goal of the current model is to calculate pH changes in the plaque leading to enamel demineralisation, several *acid–base* and *complexation equilibria* must be included together with the buffering effect of plaque by *surface charge equilibria*. Finally, a *dissolution reaction* occurs at the enamel surface due to the generated acid environment.

2.2.1. Biological reactions

Two general types of biological transformations performed by the microorganisms are included in the model: (i) the conversion of substrate and other nutrients and (ii) the production and consumption of internal storage compounds. All biological transformations considered in the model, together with their reaction stoichiometry and rate expressions are presented in Table 5. The biological rate parameters are listed in Table 6.

Glucose conversion. Glucose was chosen as substrate because it is used (directly, or indirectly under the form of sucrose) in many clinical studies (Tanzer et al., 1969; Dong et al., 1999; Pearce et al., 1999), and it is also the most readily available carbon source during prandial periods. In the model glucose is consumed by *Streptococcus* and *Actinomyces*, while *Veillonella* take up only the lactate generated in the glucose fermentation. For simplification, sucrose and its metabolic reactions were not considered in the case studies presented here, although *Streptococcus mutans* metabolises sucrose to form extracellular polymers that in part account for its enhanced cariogenicity versus non-mutans streptococci (Marsh et al., 2009).

The anaerobic glucose fermentation is the process with the highest impact on the caries formation. Depending on the environmental conditions, it occurs differently for the various organisms considered. There are two mechanisms for glucose uptake, as a function of its available concentration. The high affinity pathway is active at low glucose concentrations (i.e., during inter-prandial periods), whereas the low affinity pathway occurs at high glucose concentrations (Van der Hoeven et al., 1985; Colby and Russell, 1997). Low concentration anaerobic glucose conversion occurs with the same stoichiometry for both *Streptococcus* types (producing acetate, formate and ethanol) but the rates differ in the degree of pH inhibition (Van Beelen et al., 1986, Tables 5 and 6). *Actinomyces* is consuming low concentration glucose anaerobically by using a different metabolic pathway with formation of acetate, formate and succinate (De Jong et al., 1988). At high glucose concentrations both *Streptococcus* and *Actinomyces* are using the same pathway with production of lactate (Van Beelen et al., 1986; De Jong et al., 1988).

Since *Streptococci* and *Actinomyces* are facultative anaerobes, and oxygen may be present in a shallow superficial layer in the dental plaque exposed to saliva, the glucose can also be converted according to aerobic pathways (Table 5). The aerobic conversion of glucose is different for each of the above mentioned microorganisms, with different ratios of acetate and formate being produced (van Beelen et al., 1986; De Jong et al., 1988).

Besides the glucose taken up during meals, the model considers also a continuous low-rate production of glucose in the saliva. This process, mimics production of carbohydrate substrates (e.g., by mucin biodegradation) that feeds the resting plaque leading to a slightly acidic environment.

Storage compounds. During periods of glucose abundance *Streptococcus* and *Actinomyces* are storing substrate in the form

Table 4
Fixed chemical species and their properties.

Name	Symbol	Formula	Initial concentration	
			[kg m^{-3}]	Reference/calculation
Polyglucose in *Actinomyces*	Pgact	$(C_6H_{12}O_6)_n$	0	Assumed
Polyglucose in aciduric *Streptococcus*	Pgsta	$(C_6H_{12}O_6)_n$	0	Assumed
Polyglucose in non-aciduric *Streptococcus*	Pgstn	$(C_6H_{12}O_6)_n$	0	Assumed
Fixed charge cationic sites	SH2+	$\equiv SH_2^+$	3.59×10^{-5}	Equilibrium, $C_{S,tot}$=28.8 [kg m^{-3}], Hong and Brown (2006)
Fixed charge neutral sites	SH	$\equiv SH$	0.13	Equilibrium
Fixed charge anionic sites	S–	$\equiv S^-$	30.59	Equilibrium
Complex of fixed charge and calcium	SCa+	$\equiv SCa^+$	1.28	Equilibrium

Table 5
Stoichiometry (molar) and rates of microbial processes considered in the model dental plaque.

	Glu	O2	Suc2–	Lac–	Pro–	Ace–	For–	Eth	HCO3–	H+	H2O	Pgsta	Pgstn	Pgact	Rates	Reference
1. Anaerobic high concentration glucose fermentation																
STA	−1			2						2					$q_{m,STA,Glu,H}\ C_{STA}\ M(C_{Glu})\ I(C_{H+})$	Van Beelen et al. (1986)
STN	−1			2						2					$q_{m,STN,Glu,H}\ C_{STN}\ M(C_{Glu})\ I(C_{H+})$	Van Beelen et al. (1986)
ACT	−1			2						2					$q_{m,ACT,Glu,H}\ C_{ACT}\ M(C_{Glu})\ I(C_{H+})$	Van Beelen et al. (1986)
2. Anaerobic low concentration glucose fermentation																
STA	−1					1	2	1		3	−1				$q_{m,STA,Glu,L}\ C_{STA}\ M(C_{Glu})\ I(C_{H+})\ I(C_{O2})\ I(C_{Glu})$	Van Beelen et al. (1986)
STN	−1					1	2	1		3	−1				$q_{m,STN,Glu,L}\ C_{STN}\ M(C_{Glu})\ I(C_{H+})\ I(C_{O2})\ I(C_{Glu})$	Van Beelen et al. (1986)
ACT	−1		1			1	1		−1	3	1				$q_{m,ACT,Glu,L}\ C_{ACT}\ M(C_{Glu})\ I(C_{H+})\ I(C_{O2})\ I(C_{Glu})$	De Jong et al. (1988)
3. Aerobic glucose conversion																
STA	−1	−1				2	2			4					$q_{m,STA,Glu,L,O2}\ C_{STA}\ M(C_{Glu})\ M(C_{O2})\ I(C_{H+})\ I(C_{Glu})$	Van Beelen et al. (1986)
STN	−1	−3/2				2	1		1	4					$q_{m,STN,Glu,L,O2}\ C_{STN}\ M(C_{Glu})\ M(C_{O2})\ I(C_{H+})\ I(C_{Glu})$	Van Beelen et al. (1986)
ACT	−1	−2				2			2	4					$q_{m,ACT,Glu,L,O2}\ C_{ACT}\ M(C_{Glu})\ M(C_{O2})\ I(C_{H+})\ I(C_{Glu})$	De Jong et al. (1988)
4. Polyglucose storage																
STA	−1											1			$q_{m,STA,sto}\ C_{STA}\ M(C_{Glu})\ I(C_{H+})\ I(C_{Pgsta})$	Assumed
STN	−1												1		$q_{m,STN,sto}\ C_{STN}\ M(C_{Glu})\ I(C_{H+})\ I(C_{Pgstn})$	Assumed
ACT	−1													1	$q_{m,ACT,sto}\ C_{ACT}\ M(C_{Glu})\ I(C_{H+})\ I(C_{Pgact})$	Assumed
5. Anaerobic polyglucose conversion																
STA						1	2	1		3	−1	−1			$q_{m,STA,Pgsta}\ C_{STA}\ M(C_{Pgsta})\ I(C_{H+})\ I(C_{O2})\ I(C_{Glu})$	Similar to process (2)
STN						1	2	1		3	−1		−1		$q_{m,STN,Pgstn}\ C_{STN}\ M(C_{Pgstn})\ I(C_{H+})\ I(C_{O2})\ I(C_{Glu})$	Similar to process (2)
ACT			1			1	1		−1	3	1			−1	$q_{m,ACT,Pgact}\ C_{ACT}\ M(C_{Pgact})\ I(C_{H+})\ I(C_{O2})\ I(C_{Glu})$	Similar to process (2)
6. Aerobic polyglucose conversion																
STA		−1				2	2			4		−1			$q_{m,STA,Pgsta}\ C_{STA}\ M(C_{Pgsta})\ M(C_{O2})\ I(C_{H+})\ I(C_{Glu})$	Similar to process (3)
STN		−3/2				2	1		1	4			−1		$q_{m,STN,Pgstn}\ C_{STN}\ M(C_{Pgstn})\ M(C_{O2})\ I(C_{H+})\ I(C_{Glu})$	Similar to process (3)
ACT		−2				2			2	4				−1	$q_{m,ACT,Pgact}\ C_{ACT}\ M(C_{Pgact})\ M(C_{O2})\ I(C_{H+})\ I(C_{Glu})$	Similar to process (3)
7. Lactate fermentation																
VEL				−1	2/3	1/3			1/3	1/3					$q_{m,VEL,Lac-}\ C_{VEL}\ M(C_{Lac-})\ I(C_{H+})$	Seeliger et al. (2002)

$M(C_j) = \frac{C_j}{K_{S,X,j} + C_j}$; $I(C_j) = \frac{K_{I,X,j}}{K_{I,X,j} + C_j}$ Subscripts stand for: *S* substrate, *I* inhibition, *X* bacterial species (i.e., STA, STN, VEL or ACT) and *j* chemical species (i.e., Glu, O2, Lac–, H+, Pgsta, Pgstn, Pgact).

Table 6
Rate parameters for biological processes.

Parameter name	Symbol	Value	Reference
Substrate specific uptake rate [10^{-7} mol s^{-1} g^{-1}]	$q_{m,STA,Glu,H}$	96.70	Van der Hoeven et al. (1985)
	$q_{m,STA,Glu,L}$	5.00	Assumed as $q_{m,STN,Glu,L}$
	$q_{m,STA,Glu,L,O2}$	5.00	Assumed as $q_{m,STA,Glu,L}$
	$q_{m,STA,Pgsta,sto}$	15.6	Assumed as $q_{m,STN,Pgstn,sto}$
	$q_{m,STA,Pgsta}$	1	Assumed $0.2 \times q_{m,STA,Glu,L}$[a]
	$q_{m,STN,Glu,H}$	138	Van der Hoeven et al. (1985)
	$q_{m,STN,Glu,L}$	5.00	Van der Hoeven et al. (1985)
	$q_{m,STN,Glu,L,O2}$	5.00	Assumed as $q_{m,STN,Glu,L}$
	$q_{m,STN,Pgstn,sto}$	15.6	Hamilton (1968)
	$q_{m,STN,Pgstn}$	1	Assumed $0.2 \times q_{m,STN,Glu,L}$[a]
	$q_{m,ACT,Glu,H}$	22.00	Van der Hoeven and Gottschal (1989)
	$q_{m,ACT,Glu,L}$	0.88	Assumed $0.04 \times q_{m,ACT,Glu,H}$[b]
	$q_{m,ACT,Glu,L,O2}$	11.8	Van der Hoeven and Gottschal (1989)
	$q_{m,ACT,Pgact,sto}$	1.40	Assumed based on Komiyama et al. (1986) and Komiyama and Khandelwal (1992)
	$q_{m,ACT,Pgact}$	0.176	Assumed $0.2 \times q_{m,ACT,Glu,L}$[a]
	$q_{m,VEL,Lac-}$	252	Seeliger et al. (2002)
Substrate half-saturation constant [10^{-6} mol L^{-1}]	$K_{S,Glu,H}$	1220	Assumed based on Hamilton and Martin (1982), Van der Hoeven et al. (1985) and Dawes and Dibdin (1986)
	$K_{S,Glu,L}$	8.04	Hamilton and Martin (1982)
	$K_{S,O2}$	6.00	Van der Hoeven and Gottschal (1989)
	$K_{S,Lac-}$	290	Seeliger et al. (2002)
	$K_{S,Pgsta}$	$0.2 \times K_{S,Glu,H}$	Assumed
	$K_{S,Pgstn}$	$0.2 \times K_{S,Glu,H}$	Assumed
	$K_{S,Pgact}$	$0.2 \times K_{S,Glu,H}$	Assumed
Inhibition constant [10^{-6} mol L^{-1}]	$K_{I,STA,H+}$	15.8	Assumed[c]
	$K_{I,STN,H+}$	1.58	Assumed[d]
	$K_{I,ACT,H+}$	1.58	Assumed as $K_{I,STN,H+}$
	$K_{I,VEL,H+}$	15.8	Assumed as $K_{I,STA,H+}$
	$K_{I,STA,O2}$	0.2	Van der Hoeven and Gottschal (1989)
	$K_{I,STN,O2}$	0.2	Assumed as $K_{I,STA,O2}$
	$K_{I,ACT,O2}$	0.2	Van der Hoeven and Gottschal (1989)
	$K_{I,STA,Glu}$	2200	Assumed based on Hamilton (1968)
	$K_{I,STN,Glu}$	2200	Assumed based on Hamilton (1968)
	$K_{I,ACT,Glu}$	2200	Assumed based on Hamilton (1968)
	$K_{I,Pgsta}$	0.05	Based on Hamilton (1968)[e]
	$K_{I,Pgstn}$	0.05	Based on Hamilton (1968)[e]
	$K_{I,Pgact}$	0.05	Based on Hamilton (1968)[e]

[a] Rate value decreased to also account for slow hydrolysis of polyglucose.
[b] Assumption based on the fact that $q_{m,STA,Glu,H}/q_{m,STA,Glu,L} \approx 20$ and $q_{m,STN,Glu,H}/q_{m,STN,Glu,L} \approx 27$.
[c] Optimum pH for glycolysis in STA is 6 (Dashper and Reynolds, 1992). The reaction is assumed to be half inhibited at a pH value smaller with 1.2 units than the optimum one.
[d] Optimum pH for glycolysis in STN is 7 (Hamilton, 1968). The reaction is assumed to be half inhibited at a pH value smaller with 1.2 units than the optimum one.
[e] Microorganisms cannot store more polyglucose than 50% their cell dry weight.

of a glucose polymer, which we call here generically polyglucose. Polyglucose storage is a process inhibited at low pH (4.5) and the maximum concentration of polyglucose that can be stored equals half of the cells dry weight (Hamilton, 1968). When the glucose becomes depleted in the environment, bacteria consume the polyglucose reserves using the high affinity pathway. The model assumes the same stoichiometry for polyglucose conversion as for the equivalent low glucose concentration anaerobic and aerobic processes.

Lactate fermentation. This process is performed by *Veillonella*, and the overall expected effect is a reduction in the local acidity values, due to the lower acidity of the reaction products (acetate, propionate and bicarbonate) than reactant acidity (lactate).

2.2.2. Chemical reactions

Diverse chemical reactions can take place in the saliva, in the plaque or at the tooth surface. The model accounts for acid–base and complexation equilibria involving both mobile chemical components and fixed surface species; these reactions are treated volume-based. In addition, the enamel dissolution takes place at a solid–liquid interface, being thus treated as a surface-based reaction.

Acid–base and complexation equilibria. These equilibria are used to calculate the pH in any point of the computational domain, whether plaque or saliva. There are equilibria for the mobile dissociable chemical species, but also for the fixed charged groups on the bacterial surface. The equilibria included in the model are presented in Tables 7 and 8. All the equilibrium processes are considered to be very fast, therefore their both forward and backward reaction rate constants are assigned very large values.

Dissolution reaction. Enamel demineralisation occurs according to the stoichiometry and with the reaction rate proposed by Margolis

Table 7
Acid–base equilibria stoichiometry and rate expressions.

Reaction	Stoichiometry	Reaction rate
Water dissociation	$H2O \leftrightarrows HO- + H+$	$r_{e,H2O} = k_{H2O}\,[1-(C_{H+}\,C_{HO-})/K_{e,H2O}]$
Lactic acid dissociation	$LacH \leftrightarrows Lac- + H+$	$r_{e,LacH} = k_{LacH}\,[C_{LacH}-(C_{H+}\,C_{Lac-})/K_{e,LacH}]$
Formic acid dissociation	$ForH \leftrightarrows For- + H+$	$r_{e,ForH} = k_{ForH}\,[C_{ForH}-(C_{H+}\,C_{For-})/K_{e,ForH}]$
Acetic acid dissociation	$AceH \leftrightarrows Ace- + H+$	$r_{e,AceH} = k_{AceH}\,[C_{AceH}-(C_{H+}\,C_{Ace-})/K_{e,AceH}]$
Propionic acid dissociation	$ProH \leftrightarrows Pro- + H+$	$r_{e,ProH} = k_{ProH}\,[C_{ProH}-(C_{H+}\,C_{Pro-})/K_{e,ProH}]$
Succinic acid dissociation	$SucH \leftrightarrows Suc- + H+$	$r_{e,SucH} = k_{SucH}\,[C_{SucH}-(C_{H+}\,C_{Suc-})/K_{e,SucH}]$
Hydrogen succinate dissociation	$Suc- \leftrightarrows Suc2- + H+$	$r_{e,Suc-} = k_{Suc-}\,[C_{Suc-}-(C_{H+}\,C_{Suc2-})/K_{e,Suc-}]$
Carbonic acid dissociation	$CO2 + H2O \leftrightarrows HCO3- + H+$	$r_{e,CO2} = k_{CO2}\,[C_{CO2}-(C_{H+}\,C_{HCO3-})/K_{e,CO2}]$
Dihydrogen phosphate dissociation	$Pho- \leftrightarrows Pho2- + H+$	$r_{e,Pho-} = k_{Pho-}\,[C_{Pho-}-(C_{H+}\,C_{Pho2-})/K_{e,Pho-}]$
Dissociation cationic sites	$SH2+ \leftrightarrows SH + H+$	$r_{e,SH2+} = k_{SH2+}\,[C_{SH2+}-(C_{H+}\,C_{SH})/K_{e,SH2+}]$
Dissociation neutral sites	$SH \leftrightarrows S- + H+$	$r_{e,SH} = k_{SH}\,[C_{SH}-(C_{H+}\,C_{S-})/K_{e,SH}]$
Dissociation calcium complex	$SCa+ \leftrightarrows S- + Ca2+$	$r_{e,SCa+} = k_{SCa+}\,[C_{SCa+}-(C_{Ca2+}\,C_{S-})/K_{e,SCa+}]$
Hydroxyapatite (HAP) dissolution	$Ca_5(PO_4)_3OH + 4H+ \rightarrow 5Ca2+ + 3Pho2- + H2O$	$r_{d,HAP} = k_{en}\,(1-DS)^{2.8}(\sum C_{A(i)H})^{0.3}$, i–acids $DS = (IP \cdot K_{en})^{1/9}$ $IP = [(C_{Ca2+})^5(C_{Pho2-})^3]/(C_{H+})^4$ $K_{en} = [(K_{e,Pho2-})^3 K_{e,H2O}]/K_{HAP}$ $\sum C_{A(i)H} = C_{CO2} + C_{Pho-} + C_{LacH} + C_{AceH} +$ $+ C_{ForH} + C_{ProH} + C_{SucH} + C_{Suc-}$ $k_{en} = 0.42 \times 10^{-3}$ [min^{-1}] (Margolis and Moreno, 1992) $K_{e,Pho2-} = 10^{-12.35}$ [mol L^{-1}] (Atkins and De Paula, 2009) $K_{HAP} = 5.5 \times 10^{-55}$ [$mol^9\ L^{-9}$] (Moreno and Zahradnik, 1974)

Table 8
Rate parameters for acid–base equilibria.

Reaction	Reaction rate constant[a]	Acidity constant[b]	Reference
Water dissociation[c]	$k_{H2O} = 10^7$	$K_{e,H2O} = 10^{-14}$	Atkins and De Paula (2009)
Lactic acid dissociation	$k_{LacH} = 10^7$	$K_{e,LacH} = 10^{-3.86}$	Atkins and De Paula (2009)
Formic acid dissociation	$k_{ForH} = 10^7$	$K_{e,ForH} = 10^{-3.75}$	Atkins and De Paula (2009)
Acetic acid dissociation	$k_{AceH} = 10^7$	$K_{e,AceH} = 10^{-4.76}$	Atkins and De Paula (2009)
Propionic acid dissociation	$k_{ProH} = 10^7$	$K_{e,ProH} = 10^{-4.87}$	Atkins and De Paula (2009)
Succinic acid dissociation	$k_{SucH} = 10^7$	$K_{e,SucH} = 10^{-4.20}$	Martell and Smith (1976)
Hydrogen succinate dissociation	$k_{Suc-} = 10^7$	$K_{e,Suc-} = 10^{-5.63}$	Martell and Smith (1976)
Carbonic acid dissociation	$k_{CO2} = 10^7$	$K_{e,CO2} = 10^{-6.35}$	Atkins and De Paula (2009)
Dihydrogen phosphate dissociation	$k_{Pho-} = 10^7$	$K_{e,Pho-} = 10^{-7.21}$	Atkins and De Paula (2009)
Dissociation cationic sites	$k_{SH2+} = 10^7$	$K_{e,SH2+} = 10^{-3.45}$	Hong and Brown (2006)
Dissociation neutral sites	$k_{SH} = 10^7$	$K_{e,SH} = 10^{-4.62}$	Hong and Brown (2006)
Dissociation calcium complex	$k_{SCa+} = 10^7$	$K_{e,SCa+} = 10^{-3}$	Assumed based on Rose et al. (1993)

[a] Assumed an arbitrarily high value for very fast equilibria.
[b] The values of acidity constants are given at 25 °C. The variation with temperature from 25 °C to 37 °C was neglected.
[c] Units for rate constants are [s^{-1}] and for acidity constants are [mol L^{-1}], except for the water dissociation.

and Moreno (1992). The dissolution rate takes place when the degree of saturation (DS) of solution in contact with the tooth is less than 1, i.e., when the solution is undersaturated in respect to hydroxyapatite (HAP). Because the concentrations of phosphate (PO_4^{3-}) and hydroxyl (HO^-) ions are very low compared to those of other species, this would introduce numerical instability (scaling) in the model. These concentrations have been replaced by other species via chemical equilibria ($C_{PO4-3} = K_{e,Pho2-} \cdot C_{Pho2-}/C_{H+}$ and $C_{HO-} = K_{e,H2O}/C_{H+}$), leading to the ionic product $IP = (C_{Ca2+})^5(C_{Pho2-})^3(C_{H+})^{-4}$ and the degree of saturation $DS = (IP \cdot K_{en})^{1/9}$. The complete rate is given in Table 7.

2.3. Model domains

We are interested in the rate of tooth demineralisation, which depends on the activity (here simplified as concentration) of several chemical species at the tooth surface. These concentrations, however, can be very different from those in saliva, being the result of (bio)chemical reactions and transport processes. Because both the presence of certain reactions and transport mechanisms are different in the dental plaque and saliva, we separate these two domains (see Fig. 1). For each domain, a set of chemical and/or microbial species is defined, as well as a set of associated processes. Further, solving the mass balances for each chemical species in each of the domains will give the time-dependent concentrations of all chemical species. In the following sections detailed descriptions of every compartment will be provided.

2.3.1. Saliva

The plaque is in direct contact with a thin film of saliva present on the teeth, communicating with saliva that has not come yet into contact with the plaque. This volume of saliva not yet in contact with the plaque is named in this model "bulk saliva". The fact that saliva film and bulk saliva are into permanent contact, is leading to different concentrations in these two volumes. We calculate in this model only the change in concentrations of chemical species in the saliva film, $C_{f,j}\ (t)$. The saliva film represents only a small volume of the total saliva present in the mouth.

By assuming complete mixing in the saliva film, the mass balances for each mobile chemical species j (from Table 3) in the

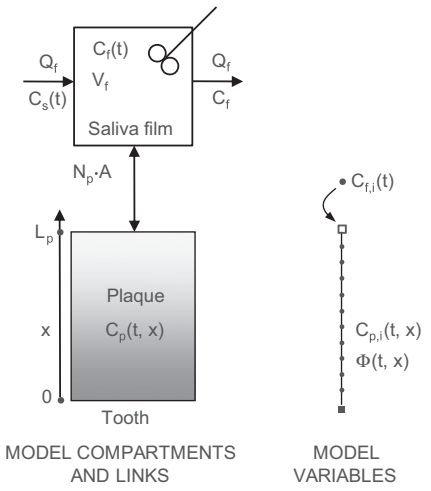

Fig. 1. The model computational domains. Saliva is represented by a film compartment on top of the dental plaque, exchanging components with the bulk saliva with the flow rate Q_f. The saliva film is perfectly mixed, having the same concentration C_f of the components over the entire volume V_f. The saliva film exchanges components with the dental plaque, with the flux N_pA. In the entire saliva domain the components concentrations (C_s in the bulk saliva and C_f in the saliva film) vary only in time, whereas in the plaque domain the concentrations C_p vary in time as well as in space (over the plaque depth L_p). The right side of the figure shows a one-dimensional representation of the plaque model: saliva and tooth are represented as boundary conditions and the plaque domain is represented as a line perpendicular to the tooth surface. The state variables for dental plaque domain (concentrations of chemical components, $C_p(t,x)$ and the electric potential, $\Phi(t,x)$) are calculated on a mesh of points, depending on the domain discretisation.

saliva film f take the general form (1):

$$\underbrace{\frac{dC_{f,j}}{dt}}_{\text{accumulation rate}} = \underbrace{\frac{Q_f}{V_f}(C_{s,j}-C_{f,j})}_{\text{exchange with the saliva bulk}} + \underbrace{\frac{A}{V_f}N_{p,j}}_{\text{exchange with plaque}} + \underbrace{R_j}_{\text{net reaction rate}} \quad (1)$$

allowing for calculation of $C_{f,j}$, the concentration of species j in the saliva film (mol m^{-3}) at each time t. The mass balance (1) is based on the species exchange with the saliva bulk represented by the input ($Q_fC_{s,j}/V_f$) and output ($Q_fC_{f,j}/V_f$) terms. There is also exchange of chemical species with the dental plaque ($N_{p,j}A/V_f$), with the flux $N_{p,j}$ calculated as the diffusive flux at the plaque–saliva interface ($x=L_p$), $D_j\partial C_{p,j}/\partial x$. Q_f is the volumetric flowrate of saliva film, V_f is the volume of saliva film, A is the area of saliva–plaque interface and $C_{s,j}$ is the concentration of species j in the saliva bulk. The saliva film compartment is characterised by a halving time $t_{h,f}=0.5$ min (Dibdin, 1990b) giving the residence time $Q_f/V_f=\ln(2)/t_{h,f}$. The plaque area per saliva volume ratio was $A/V_f=10^4$ (m^{-1}) implying that the salivary film thickness is $V_f/A=100$ μm (Fejerskov and Kidd, 2008). A series of reactions lead to the net reaction rate of each component, R_j. First, there is a constant production of glucose at very low rate in the saliva, used here to represent small amounts of carbohydrates (e.g., fucose and sialic acid) that originate from glycoproteins such as mucin (Marsh et al., 2009). Even if specifically glucose is not produced from glycoproteins, these carbohydrates are metabolisable by certain *Streptococci* and *Actinomyces*, which could explain the slightly acidic pH (~6.5) of resting plaque. The value of glucose production rate in saliva used in this model, 0.02 [mol m^{-3} s^{-1}], was calculated so that the resting pH will have the value reported in the literature (Marsh et al., 2009; Fejerskov and Kidd, 2008). Second, all the mobile components considered in the model are present in saliva, therefore acid–base equilibria are included (Table 7) with kinetic parameters presented in Table 8.

The input concentrations of mobile chemical species $C_{s,j}$ are set in several ways. For species involved in acid–base equilibria (lactate, acetate, formate, propionate, succinate, carbonate, phosphate, hydroxyl and calcium), a total concentration is given, $C_{s,j,tot}$, from which the equilibrium concentrations of each form are calculated (Table 3). The pH of secreted saliva is also set, thus $C_{s,H+}$ is known. Chemical species existing in only one form (oxygen, ethanol and chloride anion) have a fixed concentration (Table 3). The charge balancing cation (e.g., potassium) concentration is calculated from an electroneutrality condition, which must be fulfilled at any moment both in the input and in the film of saliva.

$$\sum_j z_j C_{s,j} = 0 \quad (2)$$

In order to achieve electroneutrality, two extra species are introduced in the system: cations (K+) and anions (Cl−). While the concentration of anions $C_{f,Cl-}$ is fixed, the concentration $C_{f,K+}$ is calculated from Eq. (2) based on the concentrations of all other ions present in the saliva film. For glucose, there are different types of input concentrations. In the feeding regime, $C_{s,Glu}$ was imposed to increase from zero to a maximum value of $C_{s,Glu,max}=500$ mM within $t_{step}=10$ s using a step function. This maximum concentration was maintained during the entire feeding period ($t_{feed}=2$ min). At the end of the feeding period the clearance begins, where the glucose concentration starts to decrease exponentially:

$$C_{s,Glu}(t) = C_{s,Glu}(t_{step}+t_{feed})\exp\left[-\frac{Q}{V_s}(t-(t_{step}+t_{feed}))\right] \quad (3)$$

Given the halving time in the saliva bulk compartment $t_{h,s}=2$ min (Dibdin, 1990b), the residence time can be expressed as $Q/V_s=\ln(2)/t_{h,s}$. The glucose concentration in the bulk saliva for one feeding-clearance cycle is presented in Fig. 2a.

The initial concentrations for Eq. (1) are equal with the input concentrations $C_{f,j}(0)=C_{s,j}$. The initial glucose concentration is set to a low value (Table 3).

2.3.2. Dental plaque

In the plaque domain are present all microbial groups (Table 2), all mobile chemical species (Table 3) and the fixed (immobile) chemical species (Table 4). Because microbial growth is not considered, the concentrations of microorganisms remain constant in time and have the same value throughout the plaque. The concentrations of chemical species, j, however, will change in time and also along the plaque depth, $C_{p,j}(t,x)$ (see Fig. 1).

Domain equations. Within the one-dimensional plaque domain two types of material balances were defined: for the mobile (solute) species and for the fixed chemical species. The n_j balances for mobile species (4) are Nernst–Planck equations for transport of dilute species by molecular diffusion and ion electro-migration, including also a reaction term (Newman, 1991):

$$\underbrace{\frac{\partial C_{p,j}}{\partial t}}_{\text{accumulation rate}} = \underbrace{D_j\frac{\partial^2 C_{p,j}}{\partial x^2}}_{\text{diffusion rate}} + \underbrace{D_j\frac{z_jF}{RT}\frac{\partial}{\partial x}\left(C_{p,j}\frac{\partial \Phi}{\partial x}\right)}_{\text{ion migration rate}} + \underbrace{R_{p,j}}_{\text{net reaction rate}} \quad (4)$$

where D_j is the diffusion coefficient of solute j in the plaque (at 37 °C and constant in space and time), z_j charge number, F Faraday's constant (96485 [C mol^{-1}]), R universal gas constant (8.314 [J mol^{-1} K^{-1}]) and T is the temperature (constant 310 [K]=37 [°C]).

Because immobile chemical species are either fixed on the surface of bacteria or inside them (and bacteria are also considered immobile within the plaque) their n_i material balances do

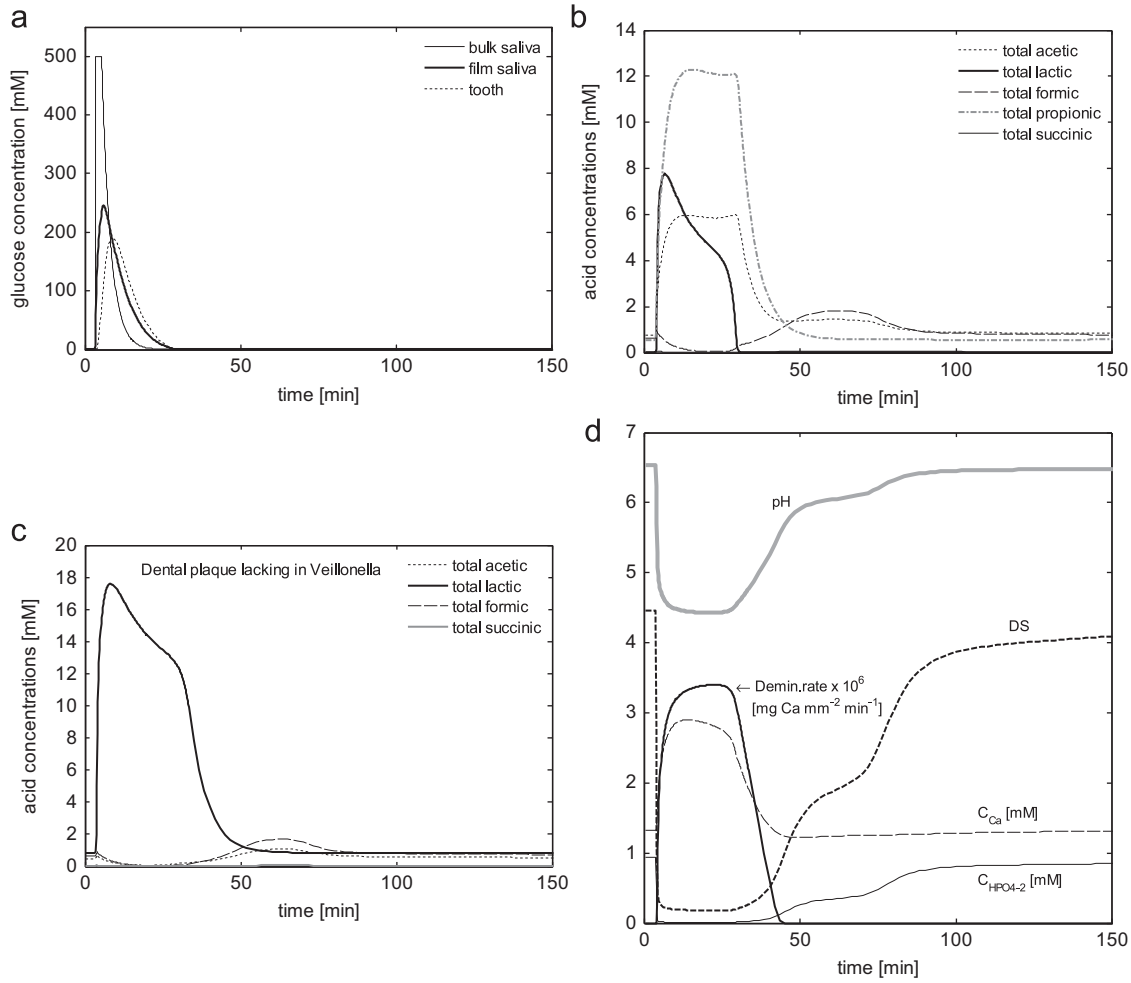

Fig. 2. (a) Variation of glucose concentration in time in the saliva bulk, saliva film and at the tooth surface (i.e., tooth–plaque interface). (b) Total (anionic and protonated) acetate, lactate, formate, propionate and succinate concentrations in time at the tooth surface. (c) Total (anionic and protonated) acetate, lactate, formate, propionate and succinate concentrations in time at the tooth surface for a dental plaque composition lacking in *Veillonella*. (d) Variation in time at the tooth surface of the main factors influencing tooth demineralisation: pH, degree of saturation (*DS*), calcium and hydrogen phosphate concentrations and demineralisation rate.

not contain any transport terms:

$$\underbrace{\frac{dC_{p,i}}{dt}}_{\substack{\text{accumulation}\\ \text{rate}}} = \underbrace{R_{p,i}}_{\substack{\text{net reaction}\\ \text{rate}}} \tag{5}$$

With $C_{p,i}(t,x)$ [mol m^{-3}] being the concentration of immobile chemical species i at a certain point x in the plaque domain.

The additional state variable $\Phi(t, x)$ in Eq. (4) is the potential field developed due to the different ion transport rates. Calculation of potential necessitates the introduction of an electroneutrality condition including both mobile and fixed charges:

$$\sum_j z_j C_{s,j} + \sum_i z_i C_{s,i} = 0 \tag{6}$$

Coupling Eqs. (4)–(6) will result in a system of (n_j+n_i+1) equations with n_j+n_i unknown concentrations and one unknown potential.

Initial conditions. The initial values of each mobile component concentrations in any point of the plaque domain are equal with those in the initial saliva composition, $C_{p,j}(0)=C_{f,j}(0)$. The initial values for storage compounds are all zero. For the surface charges, the initial concentrations result from the acid–base equilibria, given the total surface charge concentration and the total calcium concentration (Table 4). Like in saliva, the balancing mobile cations in the plaque result from a charge balance including not only the mobile but also the fixed charged species Eq. (6).

Boundary conditions. To the set of Eq. (4) two boundary conditions are attached. For the *saliva–plaque* interface (at $x=L_p$) the concentrations of all mobile chemical components are equal to those in the saliva film. At the *plaque–tooth* interface, flux conditions are implemented for all mobile species, where the molar flux due to diffusion and migration is

$$N_{pt,j} = \underbrace{D_j \frac{\partial C_{p,j}}{\partial x}}_{\substack{\text{diffusion}\\ \text{flux}}} + \underbrace{D_j \frac{z_j F}{RT} C_{p,j} \frac{\partial \Phi}{\partial x}}_{\substack{\text{ion migration}\\ \text{flux}}} \left[\text{mol m}^{-2}\ \text{s}^{-1}\right] \tag{7}$$

The molar flux of species involved in the dissolution reaction (j=H+, Ca2+, Pho2–) equals their net formation/consumption rate due to the HAP dissolution reaction (rate $r_{d,HAP}$ and stoichiometric coefficient v_j according to Table 7) calculated with concentrations at the tooth surface ($C_{pt,j}$):

$$N_{pt,j} = v_j r_{d,HAP}(C_{pt,H+}, C_{pt,Ca2+}, C_{pt,Pho2-}) \tag{8}$$

For the rest of chemical species $N_{pt,j}=0$, i.e., these do not penetrate into the tooth.

In addition, the electric potential is set to a reference value at the saliva–plaque interface ($\Phi=0$), while an electrical insulation condition is applied at the tooth surface ($\partial\Phi/\partial x=0$).

2.4. Model solution

The model was implemented in COMSOL Multiphysics software (COMSOL 4.1, Comsol Inc, Burlington, MA, www.comsol.com), which allows a very flexible and well-structured model construction and solves the resulting systems of partial differential equations by finite elements method. The plaque domain has been discretised using a uniform mesh with 5 μm size. The following solution strategy was used. First, from the initial condition the time-dependent equations were solved until no more changes occurred in concentrations of mobile species in saliva and plaque—a steady state representing a situation of resting plaque, typically encountered after maximum 2×10^4 s. Second, the simulations continued from the steady state (initial time set here to 0) for another period of 2×10^4 s. Output from the time dependent solver was taken at intervals of 10 s in the first 2000 s (i.e., during the glucose pulse disturbance and until the system roughly recovered from it) followed by intervals of 100 s until the end of the simulation. The integration time step was automatically adjusted by COMSOL so that the relative tolerance of 10^{-4} and absolute tolerance of 10^{-5} were satisfied.

3. Results and discussion

Results of the 1D plaque model were first analysed for a chosen standard case. Thereafter, the influence of different factors such as oral hygiene (e.g., plaque thickness) and eating habits on the pH change in time and tooth demineralisation were studied.

3.1. Standard case

The standard case was chosen to correspond with common situations created in clinical studies (Tanzer et al., 1969; Dong et al., 1999; Pearce et al., 1999). The dental plaque had a thickness of 500 μm. A high glucose concentration (0.5 M) is maintained for 2 min in saliva (glucose pulse), followed by oral clearance with a halving time of 2 min.

3.1.1. Glucose profiles

The imposed glucose pulse in the saliva bulk, together with the calculated glucose concentrations in the saliva film and in the plaque at the tooth surface are represented in Fig. 2(a). The glucose in the bulk saliva is cleared first (~15 min), while in the saliva film the glucose remains for a longer time (~25 min). At tooth level glucose concentrations start to decrease only after 10 min. Even if the plaque was exposed for only 2 min to high glucose concentration, glucose is present in the dental plaque for 25 min. This underlines the importance of mass transport processes (i.e., diffusion) in dental plaque when analysing caries formation.

3.1.2. Acid production

The effect of glucose presence in the microbial film is the formation of organic acids. The change in concentration of acids included in the model (acetic, lactic, formic, propionic and succinic) over time at the tooth surface is illustrated in Fig. 2(b). When considering the total concentrations of acids (sum of anionic and protonated forms) in fermenting plaque, the propionic acid (resulting from lactate consumption by *Veillonella*) is dominant, followed by acetic acid (resulting in this case mainly from lactate consumption) and lactic acid (from glucose/polyglucose fermentations). However, when only the anionic forms are considered, lactate is by far present in the highest concentration. The acid dominance in the resting plaque agrees with the results from Borgström et al. (2000) where acetate is the main component, followed by propionate and very low amounts of lactate (see Fig. 2(b), time greater than 100 min).

The total concentration of lactate/lactic acid present in the system follows the glucose pulse, reaching its maximum soon after the glucose concentration is at its highest value (around 6 min). Once the glucose concentration starts to decrease the lactate production is decreasing as well, ceasing completely once the glucose was cleared from the saliva (after ~35 min). Without production, lactate will only diffuse out of the dental plaque or be consumed by the *Veillonella*. Noticeably, even after glucose depletion lactate is still present in the plaque due to the diffusion time needed, thereby maintaining low pH values.

For a dental plaque composition without *Veillonella* (Fig. 2c), there is much more lactic acid present in the fermenting plaque (i.e., maximum 18 mM compared to 8 mM) and also for more extended period of time (i.e., ~50 min compared to ~35 min). In addition, the lactic acid is dominant in the resting plaque without *Veillonella*. In contrast, when *Veillonella* was consuming lactate (Fig. 2b), the lactate concentration was already negligible when glucose had been depleted at the tooth surface. Experimental observations (Bowden, 2000) also show that *Veillonella*'s presence in a plaque has a protective effect due to the lactic acid consumption.

Formic and succinic acids (Fig. 2b) are produced at the beginning and at the end of the feeding pulse when the glucose concentrations are low. Once the glucose is cleared, the microorganisms start to consume the stored polyglucose. Products of polyglucose degradation include mainly acetic and formic acids, whose concentrations increase after the glucose depletion. The succinate production (Fig. 2b) is very low and it only reaches negligible concentrations.

3.1.3. pH curves

The current mathematical model can reproduce the experimental Stephan curves (pH change in time) reported in the literature (Aamdal-Scheie et al., 1996; Zaura and Ten Cate (2004); Deng and Ten Cate, 2004). The model describes the three main areas of the pH curve (Fig. 2d), as observed experimentally in caries active subjects. First, the steep pH decrease at the beginning of the pulse is due to the conversion of glucose into acids. Second, a plateau area corresponding to minimum pH between 4.5 and 5 arises because of the pH inhibition on microorganisms. Finally, once most of the glucose is consumed, the pH restores to the steady state level (pH 6.5) of resting plaque. Noticeably, during the restoration period there is a short pH plateau. This second plateau corresponds to acids production from the stored polyglucose. *Veillonella*'s presence in dental plaque increases the minimum pH (Fig. 3) due its ability to consume lactic acid. Subsequently, this also reduces the time spent under critical pH. The role of storage polymers can be shown by comparing pH profiles in a plaque with and without glucose storage (Fig. 4). The consumption rate of storage compounds is very low when $pH<5.5$ and reaches the maximum only when $pH>5.5$. In consequence, storage compounds appear to have little impact on the amount of demineralised calcium because the resulted acids are mostly produced at $pH>5.5$.

3.1.4. Enamel demineralisation

The degree of saturation (*DS*) of plaque solution (at the tooth surface) in respect to HAP is the main factor affecting tooth demineralisation rate. Furthermore the *DS* is determined by pH and concentrations of calcium and hydrogen phosphate ions, all represented in Fig. 2(d). The sharp decrease of pH is immediately correlated with the *DS* fall and with a sudden increase in the demineralisation rate triggering the increase in the calcium ion

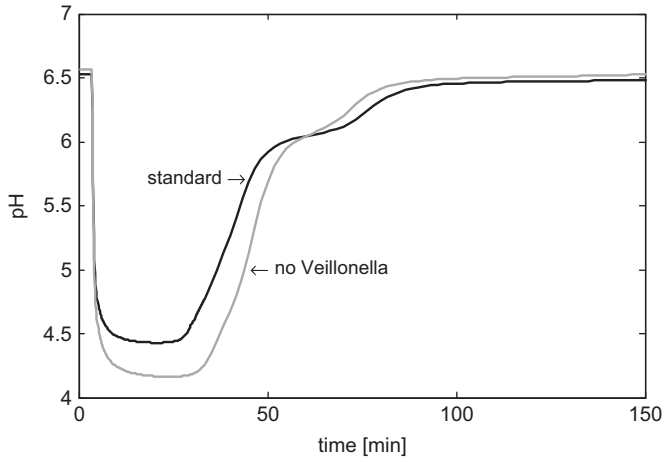

Fig. 3. Influence of *Veillonella* presence on the time-dependent pH at the tooth surface, compared to the standard case.

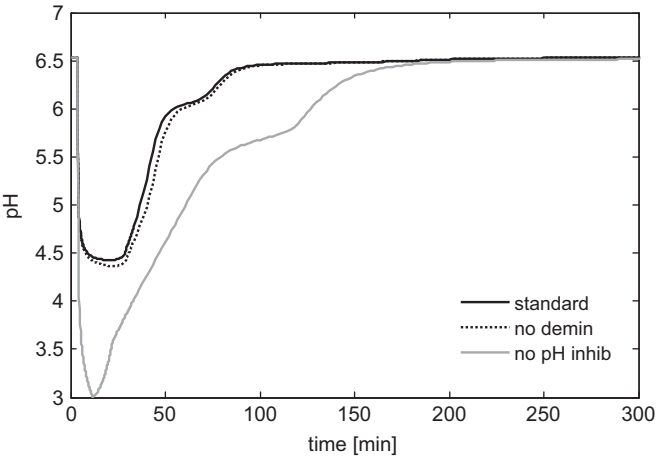

Fig. 5. Compared pH profiles at the tooth surface for the standard conditions and for cases without demineralisation and without pH inhibition.

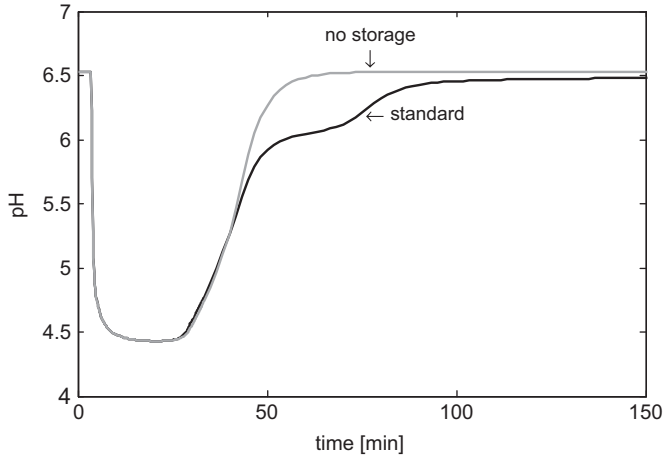

Fig. 4. Influence of storage compounds on the pH profile at tooth surface.

concentration. Model simulations show that the calcium concentration can restore to its initial level soon after the pH increases above 5.5. This is the pH value recognised to be critical for tooth enamel demineralisation (Schmidt-Nielsen, 1946). Consequently, when pH is higher than 5.5 the demineralisation stops. Importantly, the pH remains in the critical range for demineralisation long after the glucose pulse has been cleared. While glucose is cleared in about 20 min, it takes 40 min for the pH to increase above the critical level for demineralisation and 140 min to restore to the steady state (resting) value of 6.5. Overall, the amount of demineralised calcium after one acid attack obtained with this model (10^{-4} [mg Ca mm^{-2}]) is in the range experimentally observed by Margolis and Moreno (1992).

3.1.5. Effect of phosphate release on pH

A common assumption is that the plateau area of minimum pH is due to the buffering effect of the phosphate resulting from the demineralised HAP (Loesche, 1986). In order to evaluate this hypothesis, two situations have been tested, with and without demineralisation. In addition, a case without pH inhibition on microbial activity is also represented in Fig. 5. The model indicates that the buffering effect due to the demineralisation is minor, i.e., it does not change significantly the shape of Stephan curve or the minimum pH. Conversely, without acid inhibition of microbial activity the pH is decreasing abruptly not to 4.5 but further down to about 3. The pH curve has also a different shape in this case, with sharp changes in slope when the low glucose mechanism is active. Most importantly, there is no plateau area at the minimum pH. The slower pH restoration corresponding to storage compounds consumption is more extended because the polyglucose storage was not inhibited by pH either. We believe that the minimum pH plateau is better explained in the current model by pH inhibition of microbial activity and not by the buffering effect of tooth demineralisation products (e.g., phosphates).

3.1.6. Solute gradients in plaque

Unlike for the other species present in the system, the glucose concentration gradients can be very strong in the plaque especially at the beginning of glucose pulse (Fig. 6a). In the first minutes of the pulse, glucose is diffusing from the saliva towards the tooth surface while being consumed by the microorganisms. After 5 min from the beginning of the pulse the glucose concentration in the plaque becomes almost constant and it reached the maximum value at tooth surface. Then, because of salivary clearance creating low concentrations outside plaque, glucose starts to diffuse out the plaque while still being consumed by microorganisms.

The total lactate and glucose concentrations in the plaque are, as expected, correlated (see Figs. 6a and b). Almost all the glucose is converted into lactate through the high glucose fermentation pathway, as glucose penetrates in the plaque. Lactate will still be present at the tooth surface even after the glucose has been consumed (Fig. 6b). The pH value remains almost constant over the entire length of the dental plaque, except for the time at the beginning of the glucose pulse (0.5 min) when the pH value is decreasing drastically (Fig. 6c).

It is relevant to compare the levels of calcium and total phosphate concentration in the resting plaque (i.e., in steady state at 0 min) and at a time during the minimum pH period (20 min), shown in Fig. 6d. In steady state (i.e., resting plaque), the concentrations are constant over the entire plaque depth. However, when demineralisation rate is strong the calcium and phosphate concentrations are increasing at the tooth–plaque boundary and form a gradient from the tooth surface to the saliva.

3.2. Plaque thickness and area

This case study is relevant from the perspective of oral hygiene, because it could be related to tooth brushing habits. The impact of plaque thickness on the cariogenic potential is not

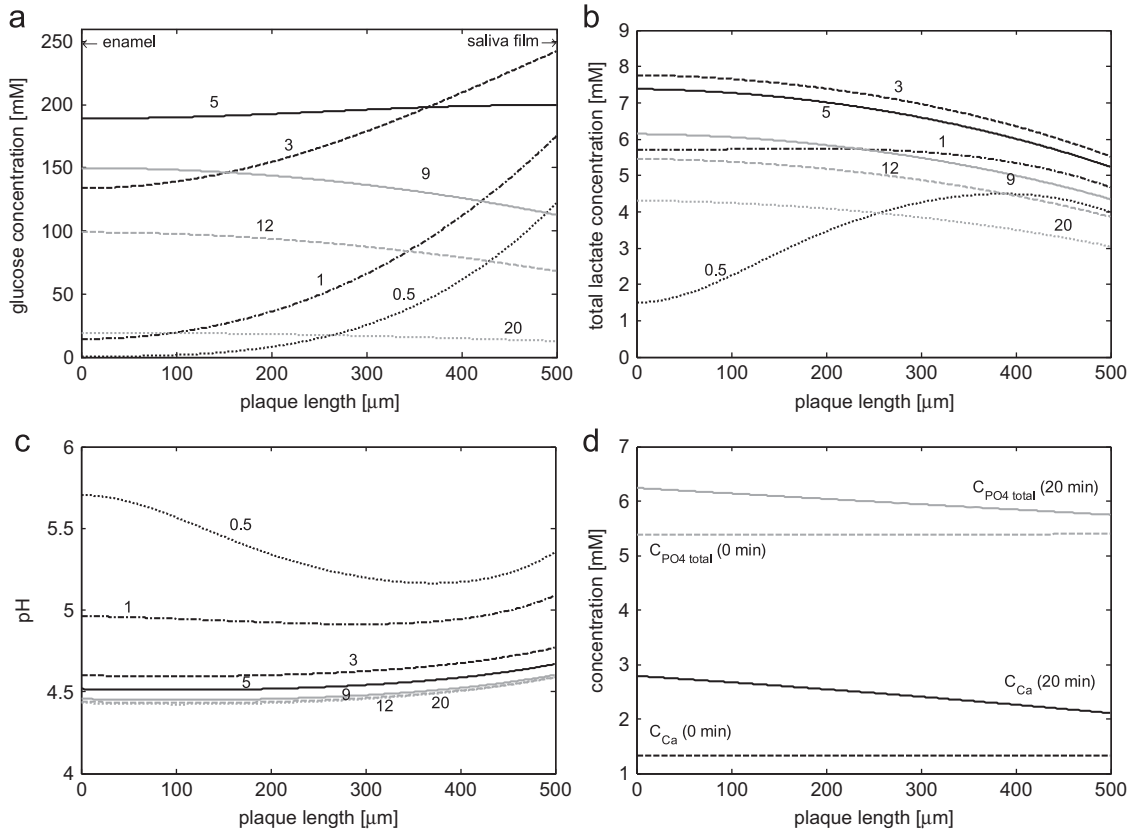

Fig. 6. Concentrations of solutes and pH along the dental plaque. Plaque length represents here the distance from enamel ($x=0$) to the plaque surface (i.e., in contact with the saliva film at $x=L_p=500$ μm): (a) glucose concentration profiles at different times: beginning of glucose pulse (0.5 min), maximum glucose pulse (1 min) and during the oral clearance (3 min, 5 min, 9 min, 12 min, 20 min). (b) Total lactate concentration profiles at different times (0.5 min, 1 min, 3 min, 5 min, 9 min, 12 min, 20 min). (c) pH profiles at different times (0.5 min, 1 min, 3 min, 5 min, 9 min, 12 min, 20 min). (d) Concentration profiles of species directly influenced by the demineralisation process: calcium and total phosphate present in the system. The profiles are represented at the initial time of the simulation (i.e., after steady state has been achieved) and after 20 min (i.e., during the minimum pH period when the rate of demineralisation is maximum).

fully understood since a variety of other factors (e.g., amount and frequency of sugars consumption, microbial composition of the plaque) are also involved. The plaque model was used to evaluate the effect of plaque thickness on the sugar induced acidification and subsequent tooth demineralisation. The pH curves were simulated with plaque thicknesses of 100 μm, 250 μm, 500 μm, and 1000 μm.

In general, the thicker the plaque the larger the negative effect of acidification. The same glucose pulse (Fig. 2a) resulted in very different pH profiles in plaque with different thicknesses (Fig. 7a). Thin plaque produced less acidification, while the pH at the tooth surface with thicker plaque reached lower values. Most importantly, not only the pH is lower but the period of critical pH is more extended for the thicker plaque. Thicker plaque progressively results in increased tooth dissolution (Fig. 7b). The calculated amount of demineralised calcium increases with the time when the plaque pH remains under the critical value of 5.5. In conclusion, this model shows a quasi-linear dependency between the mass of demineralised calcium and dental plaque thickness.

For thick plaque (i.e., 500 μm in this case) the minimum pH at the beginning of the acid attack period (e.g., 1 min, Fig. 6c) is not reached at the tooth surface, but rather closer to saliva. This suggests that for even thicker plaque (1000 μm) a secondary effect could diminish the cariogenic potential, that is, glucose consumption in shallow plaque layers. Similar model results were reported by Dibdin (Dawes and Dibdin, 1986). However, the overall impact is minor, because during most of the acid attack the pH at tooth surface is <5.5, therefore leading to demineralisation.

The tooth area covered by plaque can also have a strong impact on the Stephan curve. If only 10% of the tooth surface develops plaque of 500 μm ($a=0.1A/V_f$), then the amount of acids produced is lower. Although the pH minimum is only slightly higher than in the standard case, the period of acid attack is significantly shorter (Fig. 7c). At the same time, the resting plaque pH is also higher for smaller plaque coverage area: 6.7 instead of 6.5 in the standard case.

3.3. Drinking habits

This case study shows the importance of sugar intake patterns on the pH profiles, when the same amount of sugar is ingested. For this purpose three hypothetical regimes have been evaluated, all based on the consumption of a high (0.5 M glucose) sugar containing soft drink. The 0.5 M glucose concentration used is approximately the sugar content in most of the commercialised soft drinks, also referred to as "liquid candies" by nutritionists. The regimes were defined as follows: (1) *Thirsty*: a glass of sugar containing drink (250 mL) consumed in 15 s drinking continuously, (2) *Short-Sipping*: the same sugar containing drink consumed every minute, i.e., in 5 equal portions for 3 s (5×50 mL) at intervals of 57 s, and (3) *Long-Sipping*: the same sugar containing drink consumed every 10 min, i.e., in 5 portions for 3 s (5×50 mL) at longer intervals each (597 s).

The input glucose profiles in saliva are shown in Fig. 8(a). In both *Short-Sipping* and *Long-Sipping* cases the maximum value of glucose concentration is the same for each sip because the

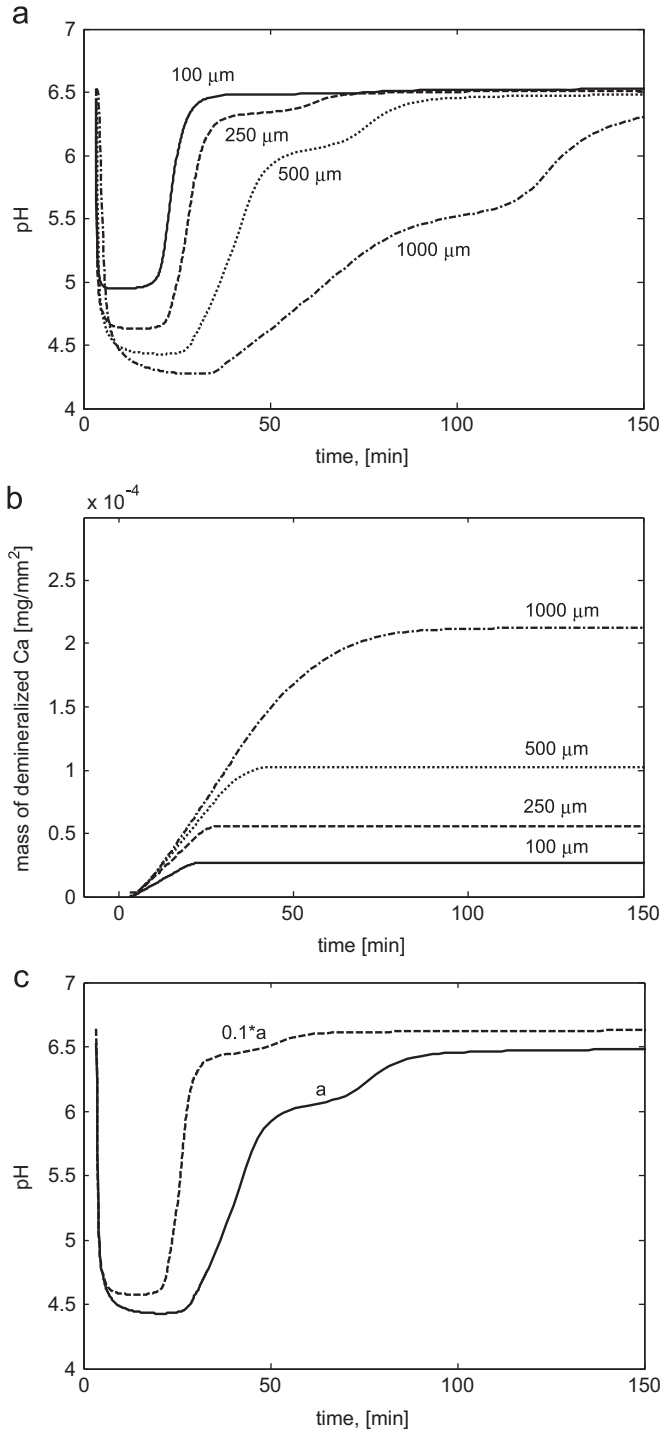

Fig. 7. (a) pH profiles at the tooth surface for different plaque thicknesses. (b) Total amount of calcium demineralised in time calculated at the tooth surface for different plaque thicknesses. (c) pH profiles at the tooth surface for different plaque areas ($a=A/V_f$ standard conditions, $0.1*a=10\%$ of the tooth surface covered with plaque).

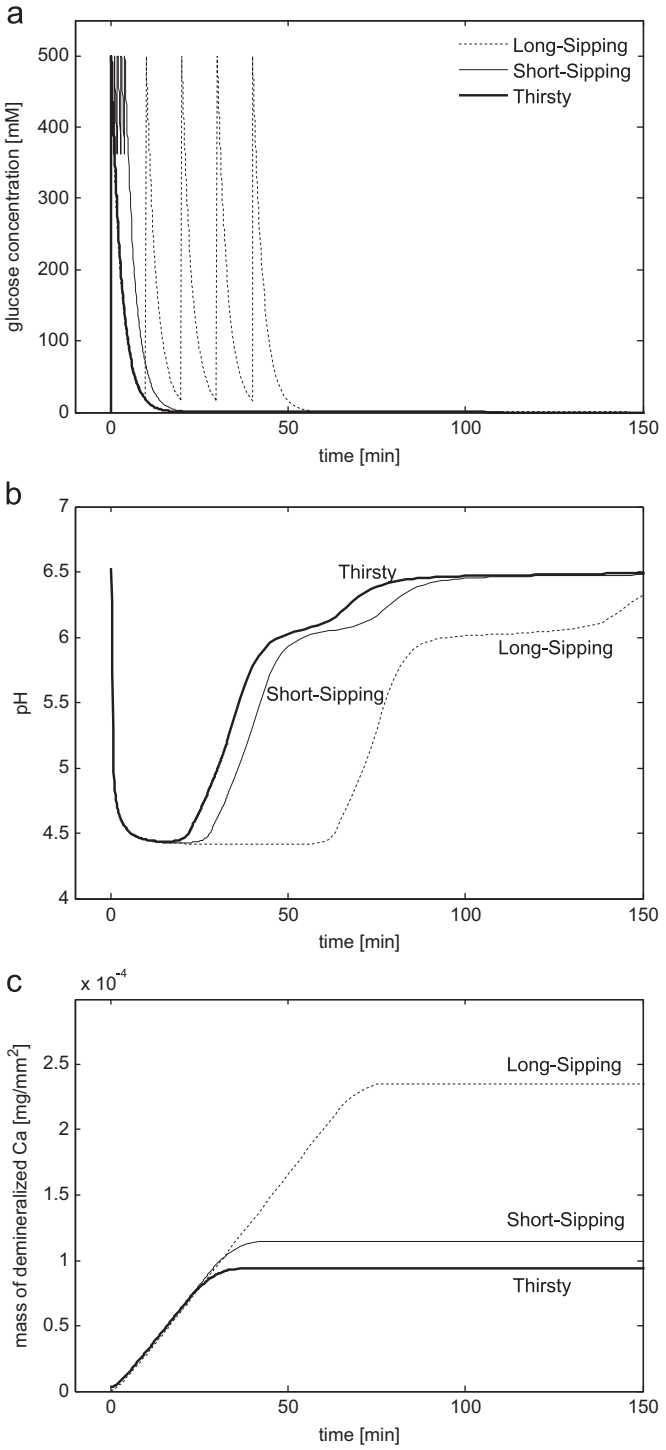

Fig. 8. (a) Variation of glucose concentration in bulk saliva in time corresponding to the three drinking patterns studied: *Thirsty*, *Short-Sipping* and *Long-Sipping*, (b) pH profiles at the tooth surface in time for three drinking patterns, and (c) total amount of calcium demineralised in time for three drinking patterns.

diluting effect of the saliva already present in the mouth was neglected. This approximation is justified because the volume of saliva present in the mouth, ca. 1 mL (Lagerlöf and Dawes, 1984), is very low compared to the 50 mL of one sip of drink.

Overall, the consumption of the sugar-containing drink over extended periods of time leads to longer times of tooth exposure to low pH. The calculated pH variations at the tooth surface in different drinking patterns for the 500 μm thick plaque are shown in Fig. 8b. Interestingly, irrespective of drinking regimes the pH minima were all found to be around 4.5, due to the pH inhibition on microbial conversions (i.e., below pH 4.5 there is no more production of acids). However, clear differences were observed when looking at the time the pH remained under the critical value for demineralisation. In the case of drink consumption every 10 min (*Long-Sipping*), the pH remained at its minimum value during the entire consumption time. Sufficient acids were

generated and remained at the tooth surface in between the consumption events, even though the glucose concentrations varied depending on the sip intervals.

By correlating the observations regarding the pH profiles with the calculated amount of calcium demineralised (Fig. 8c) it appears that the highest amount of calcium is lost in the extended drink consumption (*Long-Sipping*), when the time with pH < 5.5 at tooth surface is the longest (~75 min). These model calculations indicate that drinking a glass of sugar-containing liquid in small sips over an extended period of time has a higher cariogenic effect than drinking it at once. Furthermore, the longer the break between sips, the greater is the damage inflicted on the tooth. Noticeably, the amount of demineralised calcium during extended drinking time (*Long-Sipping* case) is the same with the amount lost for thick dental plaque (1000 μm), suggesting that a person with a good oral hygiene but bad sugar consumption habits is subjected to the same risks as a person with poor oral hygiene.

Polyglucose storage is limited by the length of the period with glucose present in the plaque, rather than by glucose concentration. In both *Short-Sipping* (Fig. 9a) and *Long-Sipping* (Fig. 9b) cases, at the time when glucose is depleted in the plaque (~30 min, respectively ~1 h) polyglucose storage also ceases. In fact, considering the assumption that microorganisms can store polyglucose up to 50% of their weight (Hamilton, 1968), and considering that in the current model the total concentration of microorganisms is 80 [kg m^{-3}], it means the theoretical maximum concentration of glycogen of 40 [kg m^{-3}] was not reached not even for the social drinking case *Long-Sipping*. The difference in the amount of stored polyglucose is reflected in the extent of the second plateau of the pH curve corresponding to the polyglucose consumption (Fig. 8b). The plateau is longer in the *Long-Sipping* case compared to *Short-Sipping* because of higher amounts of polyglucose available for consumption.

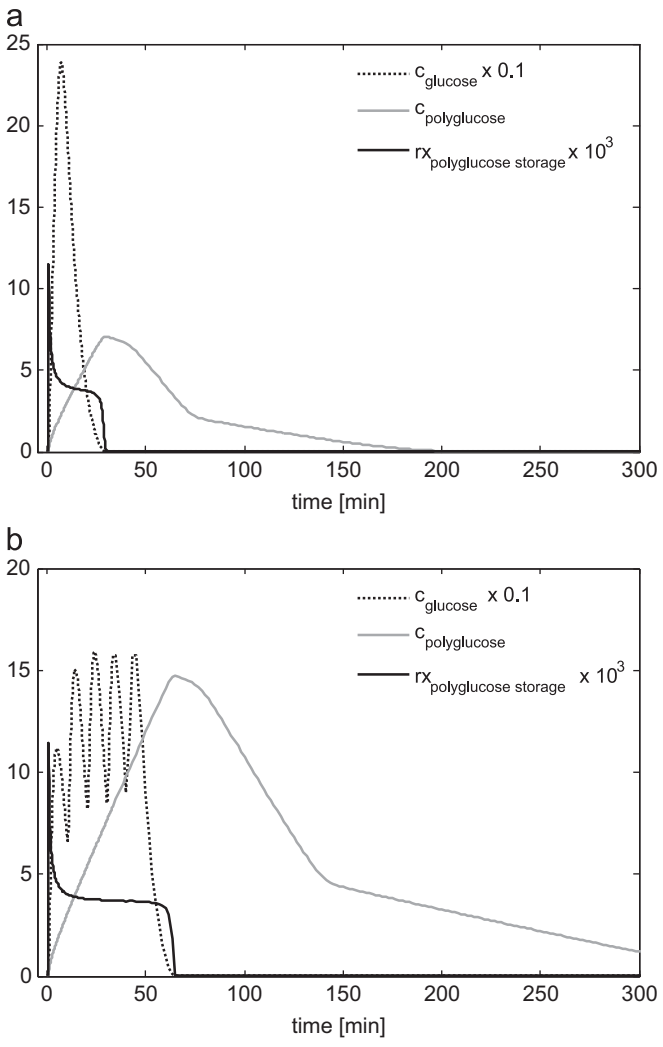

Fig. 9. Change in time of glucose concentration, total polyglucose concentration stored by all bacterial groups, and the rate of polyglucose storage by all bacterial groups at tooth surface for two studied drinking patterns (a) *Short-Sipping* and (b) *Long-Sipping*. For the purpose of easier comparison, the calculated values were scaled as follows when represented on the graph: glucose concentration was divided by 10 and polyglucose storage rate was multiplied by 1000.

Johansson et al. (2004) studied experimentally the influence of different drinking patterns on the pH at tooth surface by using an acidic drink. Their work refers to tooth erosion (i.e., dental plaque was not present) and the conditions are not identical with those used in the present model, therefore we cannot make a rigorous comparison. However, their findings could confirm that the pH profile at the tooth surface depends on the drinking pattern. Cases resembling the three drinking patterns simulated with the model led to similar pH profiles: faster recovery for Sucking case (similar to *Thirsty* case), followed by *Short-Sipping* and *Long-Sipping*.

3.4. Comparison with other models

Compared to Dibdin's work (Dawes and Dibdin, 1986; Dibdin and Wimpenny, 1999; Dibdin et al., 1995; Dibdin and Dawes, 1998), the present model introduces new aspects, such as degradation of storage compounds, mixed microbial species plaque, multiple acid production, aerobic/anaerobic metabolism and tooth demineralisation rate. The differences between the current model and the model proposed by Dawes and Dibdin (1986) are listed in Table 1.

3.4.1. Storage compounds

In the model of Dawes and Dibdin (1986) the substrate (sucrose) can be stored, but there is no further conversion of the storage compounds by microorganisms. Therefore, the process of storage is merely acting as a sink of substrate, a competitive process to glucose fermentation. This approach does not allow to study the effect of acids produced by storage compounds degradation resulting in prolonging the period of low pH under critical values for demineralisation (Zero et al., 1986). However, in the context of current model, the polyglucose degradation does not have an important impact on tooth demineralisation because it occurs at higher pH values, when demineralisation does not take place. In this situation, we can even infer that storage of glucose may have a protective effect on the tooth: the more glucose is stored, the less is available for acid formation under critical conditions (Fig. 4). Although on the short term polyglucose storage may reduce the damage, over long periods of time part of the stored polymer can be used for growth, which will result in more biomass and higher cariogenic potential (equivalent with an increase of plaque thickness).

3.4.2. Strictly anaerobic metabolism vs. aerobic and anaerobic metabolism

Previous plaque models (e.g., Dawes and Dibdin, 1986) considered that only anaerobic processes take place in dental plaque. However, because the mouth is also an aerobic environment, it seems more realistic to also include facultative aerobic conversion of glucose in the model. To test the effect of aerobic processes on the pH profiles, we compared the pH curves obtained with a thin plaque (100 μm) and thicker plaque (500 μm), in aerobic and

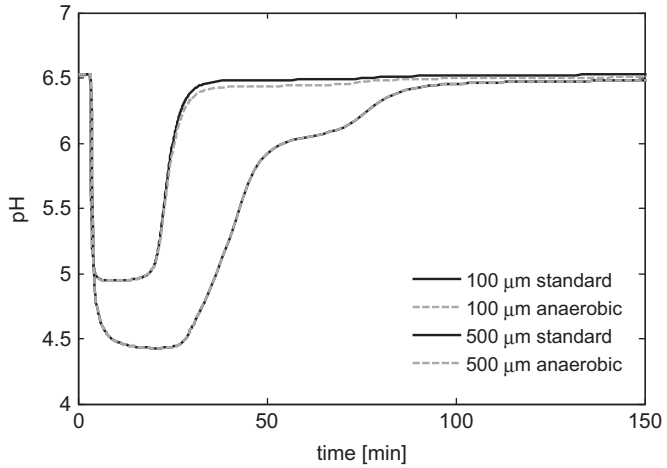

Fig. 10. pH change in time at the tooth surface for a strictly anaerobic plaque compared to the profiles obtained in the standard case for two plaque thicknesses (100 μm and 500 μm).

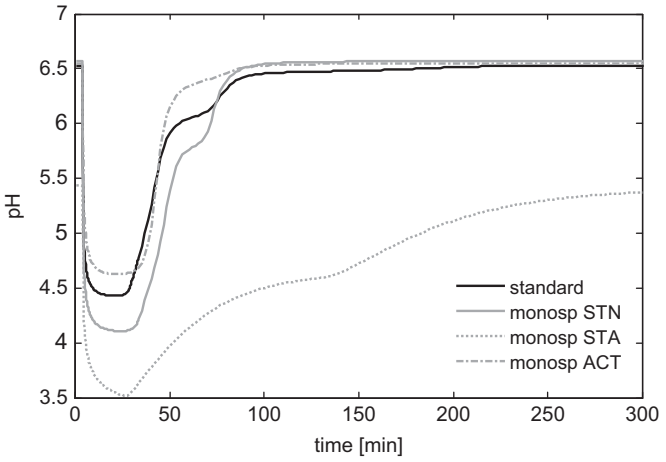

Fig. 11. pH change in time at the tooth surface, in standard case compared with three equivalent monospecies systems with only aciduric *Streptococcus* (STA), non-aciduric *Streptococcus* (STN) and *Actinomyces* (ACT), respectively.

anaerobic conditions (Fig. 10). In the thin plaque the oxygen can diffuse throughout the whole plaque depth, while the thick plaque can have both aerobic and anaerobic regions. However, model simulations indicate that the presence of oxygen has little effect on acid production and pH, because aerobic processes are producing mostly weak acids and they are inhibited at low pH. Anaerobic lactic fermentation is still the dominant generator of acidity.

3.4.3. Monospecies plaque vs. multispecies plaque

pH changes in plaque are mainly due to production of various acids during microbial fermentations. Dawes and Dibdin (1986) considered only two acids: lactic to account for strong acids and acetic as a representative of the weak acids. We proposed here more rigorous microbial process stoichiometry, including therefore other acids such as succinic, formic and propionic, together with several microbial types. Depending on the percentage of *Veillonella* present, the amount of lactic acid/lactate can vary significantly (Figs. 2b and c). Irrespective of *Veillonella*'s presence, at the time when formic acid is the dominant acid in the plaque (during storage compounds consumption) the pH is already above the critical value for demineralisation. So, even though formic acid maintains the acidic pH for longer time in plaque, this has no influence on tooth demineralisation. Depending on the model purpose (e.g., whether a strict distribution of acids is required or not, or whether detailed microbial activity is not essential) it seems reasonable to consider only lactic and acetic acids as products of microbial metabolism.

Reducing the complex ecology of the dental plaque (there are over 500 bacterial species identified so far in the dental plaque—Rosan and Lamont, 2000) to a single microbial group (Dawes and Dibdin, 1986) could be seen as a too strong model simplification. We compared the Stephan curves obtained with the standard model (multiple microbial groups) with the pH resulted when the plaque contains exclusively each of the main groups, while keeping the same total biomass concentration in the plaque (80 [kg m^{-3}]) (Fig. 11). If only *Actinomyces* (ACT) were in the plaque, the acid attack would be shorter and the pH would decrease to 4.7 only, compared to 4.5 in standard case. With only non-aciduric *Streptococci* (STN), the pH drop would be slightly more than in standard case, due to the absence of further lactic conversion by *Velionella*. However, when the plaque was containing only aciduric *Streptococci* (STA) then a minimum pH of 3.5 could be obtained and even the resting pH was below the critical value of 5.5. As expected, this would result in the strongest acid attack on the tooth enamel. Species composition could therefore indeed strongly influence the potential of caries formation.

3.5. Outlook and future model development

The model can be developed by adding different levels of complexity: new chemical and microbial components, new chemical/biological/transport processes, various other compartments or extension to two- or three-dimensional geometry.

Plaque domain: To study the influence of microbial composition on the Stephan curve, other potentially important microbial groups (e.g., *Lactobacillus*) could be added. In addition, the bacterial composition should develop in time by including growth of several microbial groups in the biofilm (as in other biofilm models, e.g., Wanner and Gujer, 1986). Together with growth, microbial decay or inactivation could be included.

If acidity decreasing compounds (e.g., urea, arginine, ammonium) and the processes in which these are involved are taken into account, then the minimum pH should be at least half a pH unit higher as shown by Dibdin and Dawes (1998).

Saliva domain: In order to account for different salivary composition function of the tooth's position in the mouth, saliva flow over the tooth surface should be included. This would help evaluating if the increased saliva flow during meals does not only help the digestion, but has also a protective effect on the tooth during a cariogenic challenge.

Tooth: For a more realistic representation of the total amount of HAP lost during feeding/resting cycles, tooth remineralisation should also be included.

In order to study the evolution of caries profile in time, i.e., variation of the HAP content in depth of the tooth, a separate computational domain representing the tooth has to be added.

An important addition to the current model (suggested also by Dibdin and Wimpenny, 1999), would be the two-dimensional geometry in order to account for the pH gradients along the tooth–plaque interface and for a better representation of microbial competition for space within the plaque. A two- or three-dimensional approach would also allow considering the localised effect of dental plaque on the tooth and simulation of caries formation on different places on the tooth.

4. Conclusions

In the current paper we describe a one-dimensional numerical model of dental plaque. The model simulates the pH variation (i.e., the so-called Stephan curve) under the influence of microbial metabolism occurring in dental plaque, followed by the tooth demineralisation at $pH < 5.5$. Using the current model several hypothesis have been tested:

(1) Poor oral hygiene (having as consequence a thick dental plaque) leads to caries development. Model results confirm that for thicker plaque the amount of demineralised HAP is higher than for thinner plaque.
(2) Consumption of small amounts of sweets extended over long periods of time leads to tooth decay. When studying different drinking behaviours it appears that slow social drinking (the so called *Long-Sipping* in the current model) is the most harmful from all the tested patterns, especially when compared with the *Thirsty* case. The amount of demineralised calcium in the *Long-Sipping* case is similar to the case of poor oral hygiene (i.e., 1000 μm dental plaque thickness) when the same amount of glucose is consumed at once.
(3) The presence of bacterial storage compounds may not have a direct harmful effect on the teeth by extending the period of acid attack because these compounds are metabolised to acids only when the pH had been restored above 5.5.
(4) The presence of *Veillonella* in dental plaque has a protective effect due to its ability to consume lactic acid and convert it in weaker acids and the effect is stronger at higher percentage of *Veillonella* in the dental plaque.

This model is a good base for future developments, such as: including the changes of microbial composition in time, plaque growth and decay, tooth remineralisation, extensions to two- or three-dimensional geometries, or saliva flow over the tooth and plaque.

Acknowledgements

This work was financially supported by the Netherlands Organization for Scientific Research (NWO, VIDI grant 864.06.003).

References

Aamdal-Scheie, A., Luan, W.-M., Dahlén, G., Fejerskov, O., 1996. Plaque pH and microflora of dental plaque on sound and carious root surfaces. J. Dent. Res. 75 (11), 1901–1908.
Atkins, P., De Paula, J., 2009. Physical Chemistry, 9th ed W.H. Freeman.
Borgström, M.K., Edwardsson, S., Sullivan, Å., Svensäter, G., 2000. Dental plaque mass and acid production activity of the microbiota on teeth. Eur. J. Oral Sci. 108, 412–417.
Bowden, G.H.W., 2000. The microbial ecology of dental caries. Microb. Ecol. Health D 12, 138–148.
Colby, S.M., Russell, R.R.B., 1997. Sugar metabolism by mutans streptococci. J. Appl. Microbiol. Symp. Suppl. 83, 80S–88S.
Cussler, E.L., 1984. Diffusion: Mass Transfer in Fluid Systems, 1st ed. Cambridge University Press.
Cussler, E.L., 2009. Diffusion: Mass Transfer in Fluid Systems, 3rd ed. Cambridge University Press.
Dashper, S.G., Reynolds, E.C., 1992. pH regulation by *Streptococcus mutans*. J. Dent. Res. 71, 1159–1165.
Dawes, C., 1989. An analysis of factors influencing diffusion from dental plaque into a moving film of saliva and the implications for caries. J. Dent. Res. 68 (11), 1483–1488.
Dawes, C., Dibdin, G.H., 1986. A theoretical analysis of the effects of plaque thickness and initial salivary succrose concentration on diffusion of succrose into dental plaque and its conversion to acid during salivary clearance. J. Dent. Res. 65 (2), 89–94.
De Jong, M.H., Van der Hoeven, J.S., Van den Kieboom, C.W.A., Camp, P.J.M., 1988. Effects of oxygen on the growth and metabolism of *Actinomyces viscous*. FEMS Microbiol. Ecol. 53, 45–52.
Deng, D.M., Ten Cate, J.M., 2004. Demineralization of dentin by *Streptococcus mutans* biofilms grown in the constant depth film fermentor. Caries Res. 38, 54–61.
Dibdin, G.H., 1990a. Plaque fluid and diffusion: study of the cariogenic challenge by computer modelling. J. Dent. Res. 69 (6), 1324–1331.
Dibdin, G.H., 1990b. Effect on a cariogenic challenge of saliva/plaque exchange via a thin salivary film studied by mathematical modelling. Caries Res. 24, 231–238.
Dibdin, G.H., 1997. Mathematical modelling of biofilms. Adv. Dent. Res. 11 (1), 127–132.
Dibdin, G.H., Dawes, C., 1998. A mathematical model of the influence of salivary urea on the pH of fasted dental plaque and on the changes occurring during a cariogenic challenge. Caries Res. 32, 70–74.
Dibdin, G.H., Reece, G.L., 1984. Computer simulation of diffusion with reaction in dental plaque. Caries Res. 18 (2), 191–192.
Dibdin, G.H., Wimpenny, J., 1999. Steady state biofilm: practical and theoretical models. Method Enzymol. 310, 296–322.
Dibdin, G.H., Dawes, C., Macpherson, L.M.D., 1995. Computer modelling of the effects of chewing sugar-free and sucrose-containing gums on the pH changes in dental plaque associated with a cariogenic challenge at different intra-oral sites. J. Dent. Res. 74 (8), 1482–1488.
Dong, Y.-M., Pearce, E.I.P., Yue, L., Larsen, M.J., Gao, X.-J., Wang, J.-D., 1999. Plaque pH and associated parameters in relation to caries. Caries Res. 33, 428–436.
Featherstone, J.D.B., Duncan, J.F., Cutress, T.W., 1979. A mechanism for dental caries based on chemical processes and diffusion phenomena during in vitro caries simulation on human tooth enamel. Arch. Oral Biol. 24, 101–112.
Fejerskov, O., Kidd, E., 2008. Dental Caries: The Disease and its Clinical Management, 2nd ed Blackwell Munksgaard.
Filoche, S., Wong, L., Sisson, C.H., 2010. Oral biofilms: emerging concepts in microbial ecology. J. Dent. Res. 89 (1), 8–18.
Fox, J.L., Higuchi, W.I., Fawzi, M.B., Wu, M.-S., 1978. A new two-site model for hydroxyapatite dissolution in acidic media. J. Colloid Interface Sci. 67 (2), 312–330.
Hamilton, I.R., 1968. Synthesis and degradation of intracellular polyglucose in *Streptococcus salivarius*. Can. J. Microbiol. 14 (1), 65–77.
Hamilton, I.R., Buckley, N.D., 1991. Adaptation by *Streptococcus mutans* to acid tolerance. Oral Microbiol. Immunol. 6 (2), 65–71.
Hamilton, I.R., Martin St., E.J., 1982. Evidence for the involvement of proton motive force in the transport of glucose by a mutant of *Streptococcus mutans* Strain DR0001 defective in glucose-phosphoenolpyruvate phosphotransferase activity. Infect. Immun. 36 (2), 567–575.
Higuchi, W.I., Young, F., Lastra, J.L., Koulourides, T., 1970. Physical model for plaque action in the tooth–plaque–saliva system. J. Dent. Res. 49, 47–60.
Hojo, K., Nagaoka, S., Ohshima, T., Maeda, N., 2009. Bacterial interactions in dental biofilm development. J. Dent. Res. 88 (11), 982–990.
Holly, F.J., Gray, J.A., 1968. Mechanism for incipient carious lesion growth utilizing a physical model based on diffusion concepts. Arch. Oral Biol. 13, 319–334.
Hong, Y., Brown, D.G., 2006. Cell surface acid–base properties of *Escherichia coli* and *Bacillus brevis* and variation as a function of growth phase, nitrogen source and C:N ratio. Colloid Surf. B 50, 112–119.
Johansson, A.-K., Lingström, P., Imfeld, T., Birkhed, D., 2004. Influence of drinking method on tooth surface pH in relation to dental errosion. Eur. J. Oral Sci. 112, 484–489.
Komiyama, K., Khandelwal, R.L., 1992. Acid production by *Actinomyces viscosus* of root surface caries and non-caries origin during glycogen synthesis and degradation at different pH levels. J. Oral Pathol. Med. 21 (8), 343–347.
Komiyama, K., Khandelwal, R.L., Duncan, D.E., 1986. Glycogen synthetic abilities of *Actinomyces viscosus* and *Actinomyces naeslundii* freshly isolated from dental plaque over root surface caries lesions and non-carious sites. J. Dent. Res. 65 (6), 899–902.
Lagerlöf, F., Dawes, C., 1984. The volume of saliva in the mouth before and after swallowing. J. Dent. Res. 63, 618–621.
Larsen, M.J., Pearce, E.I.F., 1992. Some notes on the diffusion of acidic and alkaline agents into natural human caries lesions in vitro. Arch. Oral Biol. 37 (5), 411–416.
Lippert, F., Parker, D.M., Jandt, K.D., 2004. In vitro demineralization/remineralization cycles at human tooth enamel surfaces investigated by AFM and nanoindentation. J. Colloid Interface Sci. 280, 442–448.
Loesche, W.J., 1986. Role of *Streptococcus mutans* in human dental decay. Microbiol. Rev. 50 (4), 353–380.
Margolis, H.C., Moreno, E.C., 1992. Kinetics of hydroxyapatite dissolution in acetic, lactic and phosphoric acid solutions. Calcif. Tissue Int. 50, 137–143.
Marsh, P.D., Martin, M.V., Lewis, M.A.O., Williams, D.W., 2009. Oral Microbiology, 5th ed Churchill Livingstone Elsevier.
Martell, A.E., Smith, R.M., 1976. Critical Stability Constants, vols. 1–4. Plenum Press, New York.
Moreno, E.C., Zahradnik, R.T., 1974. Chemistry of enamel subsurface demineralization in vitro. J. Dent. Res. 53 (2), 226–235.
Newman, J.S., 1991. Electrochemical Systems, 2nd ed Prentice-Hall.
Pearce, E.I.F., Margolis, H.C., Kent Jr., R.L., 1999. Effect of in situ plaque mineral supplementation on the state of saturation of plaque fluid during sugar-induced acidogenesis. Eur. J. Oral Sci. 107, 251–259.
Ritz, H.L., 1967. Microbial population shifts in developing human dental plaque. Arch. Oral Biol. 12, 1561–1568.
Rosan, B., Lamont, R.J., 2000. Dental plaque formation. Microbes Infect. 2, 1599–1607.
Rose, R.K., Dibdin, G.H., Shellis, R.P., 1993. A quantitative study of calcium binding and aggregation in selected oral bacteria. J. Dent. Res. 72 (1), 78–84.
Schmidt-Nielsen, B., 1946. The solubility of tooth substance in relation to the composition of saliva. Acta Odontol. Scand. 7 (Suppl. 2), 1–88.

Seeliger, S., Janssen, P.H., Schink, B., 2002. Energetics and kinetics of lactate fermentation to acetate and propionate via methylmalonyl-CoA or acrylyl-CoA. FEMS Microbiol. Lett. 211, 65–70.

Shellis, R.P., Dibdin, G.H., 1988. Analysis of the buffering systems in dental plaque. J. Dent. Res. 67 (2), 438–446.

Takahashi, N., Nyvad, B., 2008. Caries ecology revisited: microbial dynamics and the caries process. Caries Res. 42, 409–418.

Tanzer, J.M., Krichevsky, M.I., Keyes, P.H., 1969. The metabolic fate of glucose catabolized by a washed stationary phase caries-conductive *Streptococcus*. Caries Res. 3, 167–177.

Ten Cate, J.M., 1982. A model for enamel lesion remineralisation. In: Leach, S.A., Edgar, W.M. (Eds.), Demineralization and Remineralization of the Teeth. Proceedings of a workshop, Samos, Greece, IRL Press Ltd., Oxford, England, October 11–15, pp. 129–144.

Van Beelen, P., Van der Hoeven, J.S., De Jong, M.H., Hoogendoorn, H., 1986. The effect of oxygen on the growth and acid production of *Streptococcus mutans* and *Streptococcus sanguis*. FEMS Microbiol. Ecol. 38, 25–30.

Van Dijk, J.W.E., Borggreven, J.M.P.M., Driessens, F.C.M., 1979. Chemical and mathematical simulations of caries. Caries Res. 13, 169–180.

Van der Hoeven, J.S., Gottschal, J.C., 1989. Growth of mixed cultures of *Actinomyces viscosus* and *Streptococcus mutans* under dual limitation of glucose and oxygen. FEMS Microbiol. Ecol. 62, 275–284.

Van der Hoeven, J.S., De Jong, M.H., Camp, P.J.M., Van den Kieboom, C.W.A., 1985. Competition between oral *Streptococcus* species in the chemostat under alternating conditions of glucose limitation and excess. FEMS Microbiol. Ecol. 31, 373–379.

Van der Hoeven, J.S., van den Kieboom, C.W.A., Camp, P.J.M., 1990. Utilization of mucin by oral *Streptococcus* species. Antonie Van Leeuwenhoek Int. J. Gen. 57 (3), 165–172.

Vaný́sek, P., 2001. Handbook of Chemistry and Physics, 82nd ed CRC Press LLC, Boca Raton, pp. 5–95, 6–194.

Wanner, O., Gujer, W., 1986. A multispecies biofilm model. Biotechnol. Bioeng. 28, 314–328.

Zaura, E., Ten Cate, J.M., 2004. Dental plaque as a biofilm: a pilot study of the effects of nutrients on plaque pH and dentin demineralization. Caries Res. 38 (Suppl. 1), 9–15.

Zero, D.T., van Houte, J., Russo, J., 1986. Enamel demineralization by acid produced from endogenous substrate in oral *Streptococci*. Arch. Oral Biol. 31 (4), 229–234.

Zimmerman, S.O., 1966a. A mathematical theory of enamel solubility and the onset of dental caries: I. The kinetics of dissolution of powdered enamel in acid buffer. Bull. Math. Biophys. 28, 417–432.

Zimmerman, S.O., 1966b. A mathematical theory of enamel solubility and the onset of dental caries: II. Some solubility equilibrium considerations of hydroxyapatite. Bull. Math. Biophys. 28, 433–441.

Zimmerman, S.O., 1966c. A mathematical theory of enamel solubility and the onset of dental caries: III. Development and computer simulation of a model of caries formation. Bull. Math. Biophys. 28, 443–464.